Bases moleculares de la apoptosis inducida por drogas en neoplasias linfoides

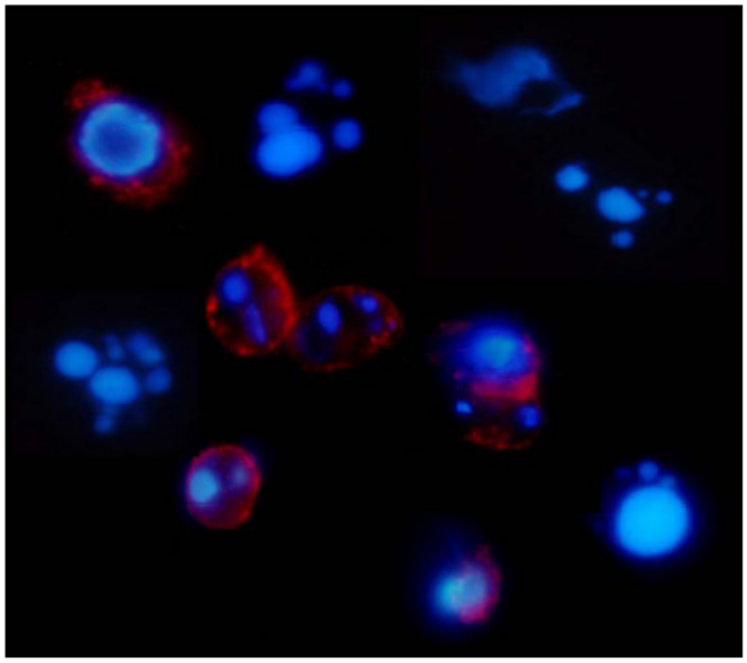

Silvia Marcé Torra

Facultat de Medicina
Universitat de Barcelona

ANEXO

Participación en otros trabajos en el marco de los síndromes linfoproliferativos crónicos y relacionados con el tema de esta tesis:

Martinez A, Bellosillo B, Bosch F, Ferrer A, **Marcé S**, Villamor N, Ott G, Montserrat E, Campo E, Colomer D. Nuclear survivin expresión in mantle cell lymphoma is associated with cell proliferationand survival. Am J Pathol 2004; 164 (2): 501- 510.

Crespo M, Bosch F, Villamor N, Bellosillo B, Colomer D, Rozman M, **Marcé S**, López-Guillermo A, Campo E, Montserrat E. ZAP-70 expression as a surrogate for immunoglobulin-variable-region mutations in chronic lymphocytic leukemia. N Engl J Med 2003; 348 (18): 1764- 1775.

Bellosillo B, Villamor N, López-Guillermo A, **Marcé S**, Bosch F, Campo E, Montserrat E, Colomer D. Spontaneous and drug-induced apoptosis is mediated by conformational changes of Bax and Bak in B-cell chronic lymphocytic leukemia. Blood 2002; 100 (5): 1810- 1816.

Bellosillo B, Villamor N, López-Guillermo A, **Marcé S**, Esteve J, Campo E, Colomer D, Montserrat E. Complement-mediated cell death induced by rituximab in B-cell lymphoproliferative disorders is mediated in vitro by a caspase-independent mechanism involving the generation of reactive oxygen species. Blood 2001; 98 (9): 2771- 2777.

American Journal of Pathology, Vol. 164, No. 2, February 2004

Nuclear Survivin Expression in Mantle Cell Lymphoma Is Associated with Cell Proliferation and Survival

Antonio Martinez,* Beatriz Bellosillo,* Francesc Bosch,† Ana Ferrer,† Silvia Marcé,* Neus Villamor,* German Ott,‡ Emili Montserrat,† Elias Campo,* and Dolors Colomer*

From the Hematopathology Unit, Department of Pathology, and Department of Hematology,† Hospital Clínic, Institut d'Investigacions Biomèdiques August Pi i Sunyer (IDIBAPS), University of Barcelona, Barcelona, Spain; and Institute of Pathology,‡ University of Würzburg, Würzburg, Germany*

Survivin is a member of the inhibitor of apoptosis protein family that is expressed in G2/M phase. Survivin is overexpressed and associated with parameters of poor prognosis in different human tumors. The role of survivin in the pathogenesis of mantle cell lymphoma (MCL) was examined in a series of typical and blastoid tumors. Survivin was detected as a nuclear pattern in a variable number of tumor cells. Mitotic figures were always positive with a strong delineation of the chromosomes. Western blot analysis confirmed the presence of survivin only in nuclear fractions. Protein expression detected by immunohistochemistry correlated with mRNA levels analyzed by quantitative real-time reverse transcription-polymerase chain reaction ($P < 0.0001$). Survivin expression levels were higher in blastoid MCL variants ($P < 0.0001$) and were associated with the proliferative activity ($P = 0.001$), but not with the ploidy status of the tumors. The number of apoptotic cells was independent of survivin or Ki-67 expression. Overall survival was significantly shorter in patients with high survivin expression. However, in a multivariate analysis, proliferative index was a better predictor of survival than survivin score. These findings indicate that survivin is commonly expressed in MCL with a nuclear and mitotic pattern. The expression levels are strongly associated with the proliferative activity of the tumors and the survival of the patients, suggesting a potential role in cell cycle regulation and tumor progression. ***(Am J Pathol 2004, 164:501–510)***

Mantle cell lymphoma (MCL) is a malignant lymphoproliferative disorder characterized by the proliferation of CD5+, CD23- monoclonal B cells containing the chromosomal translocation t(11;14)(q13;q32) which places the cyclin D1 gene under the transcriptional control of the immunoglobulin heavy chain enhancer elements.[1,2] Additional alterations in the tumor suppressor genes p16INK4a and p53 have been described in aggressive variants of MCL, suggesting that these genes may cooperate with cyclin D1 activation in the progression of these lymphomas.[3–6] Classical cytogenetic and comparative genomic hybridization (CGH) studies have also demonstrated complex karyotypes and high number of additional recurrent chromosomal imbalances.[7–9] Furthermore, a high incidence of tetraploidy has been described in blastoid variants of MCL.[10] This high number of secondary chromosomal aberrations are associated with inactivation of DNA damage response genes such as ATM and CHK2.[11,12] MCL has an aggressive clinical course, with a median survival of less than 5 years, and a poor response to conventional treatments. The mechanisms accounting for the resistance of these tumor cells to chemotherapeutic drugs are poorly understood. It has been postulated that most chemotherapeutic agents induce cell death by apoptosis triggering,[13] but the molecular basis for chemoresistance in this pathology is not well known.

Inhibitors of apoptosis proteins (IAP) are a family of negative regulators of apoptosis.[14] Survivin is a unique mammalian IAP family protein that is expressed during mitosis in a cell-cycle-dependent manner and localized to different components of the mitotic apparatus.[15,16] Survivin is virtually undetectable in most normal adult tissues, but it is highly expressed during embryogenesis and in most human cancers. This overexpression in malignant tumors has been associated with an aggressive behavior and poor prognosis of the patients.[17–20] The anti-apoptotic function and topographic distribution during cell cycle progression have suggested that survivin may play a role in the mitotic checkpoint control, regulat-

Supported in part by grants FIS 00/946, and 03-398 European Union European Framework 5 grant QLG1-CT-2000–0687, CICYT SAF 02–3261, Asociación Española contra el Cancer (AECC) and FIJC-02/P-EM and P-CR. A.M. had a fellowship from Hospital Clínic and Fondo de Investigacion Sanitaria (FIS) and B.B. was the recipient of a research fellowship from the Instituto de Salud Carlos III.

A.M. and B.B. contributed equally to this study.

Accepted for publication October 18, 2003.

Address reprint requests to Elias Campo, Hematopathology Unit, Department of Pathology, Hospital Clinic, Villarroel 170, 08036 Barcelona, Spain. E-mail: campo@medicina.ub.es.

Table 1. Immunohistochemical Study: Antibodies and Conditions of Usage

Antibody	Source	Dilution	Antigen retrieval*			
			Buffer	pH	Time	Temperature
Survivin	Novus	1:1000	Cytrate	6	5 min	100°C
Cleaved caspase-3	Cell Signaling	1:10	EDTA	8	2 min	100°C
Ki-67 (MIB-1)	Immunotech	1:400	Cytrate	6	5 min	100°C

ing chromosome segregation and cell division.[21,22] Its overexpression in cancer cells may facilitate tumor progression by providing a mechanism to tolerate increasing chromosomal abnormalities and promoting resistance to treatment with anticancer drugs and irradiation.[19,20]

The aim of this study was to determine the potential role of survivin in the pathogenesis of MCL, analyzing the relationship of its expression with the proliferative activity, genomic alterations, apoptotic levels of the tumors, as well as response to therapy and survival of the patients.

Materials and Methods

Patients

Tumor specimens from 80 patients diagnosed with MCL between 1988 and 2000 were obtained from the Department of Pathology of the Hospital Clinic, University of Barcelona (Spain) and the Institute of Pathology, University of Würzburg (Germany). Tumors were classified as classical MCL (n = 57; 71%), and blastoid variant, including pleomorphic (n = 9; 11%) and blastic (n = 14; 18%) subtypes.[1,23] In addition, paired samples from two patients that had progressed from classical to blastoid MCL variants (5 months to 45 months for progression) and 10 paired samples from 5 classical MCL at different times of disease (15 months to 68 months of follow-up) were also examined. The immunophenotype of the tumors was analyzed by immunohistochemistry on tissue sections and/or by flow cytometry on cell suspensions. Cyclin D1 overexpression was demonstrated in all cases by Northern blot analysis and/or immunohistochemistry.

For each patient the following initial data were recorded and evaluated for analysis: 1) clinical data: age, sex, performance status (PS) according to the Eastern Cooperative Oncology Group (ECOG) scale, and presence of B-symptoms; 2) hematological and biochemical parameters: Hb, WBC count, presence of atypical lymphocytes in peripheral blood, platelet count, serum β2-microglobulin, and serum LDH level; 3) tumor extension data: number of nodal and extranodal involved sites, spleen palpable below the left costal margin, hepatomegaly, Ann Arbor stage, and bone marrow infiltration; and 4) the International Prognostic Index (IPI), as defined by the International Non-Hodgkin's Lymphoma Prognostic Factors Project.[24] Moreover, response to treatment and survival, measured from the time the sample was obtained, was also recorded and analyzed.

Cell Lines

The following human cell lines were used: Raji and Daudi, derived from a Burkitt lymphoma and Granta 519, derived from a MCL. Cell lines were purchased from the American Type Culture Collection (ATCC) and were cultured in RPMI 1640 medium (Gibco BRL, Paisley, Scotland) containing 10% heat-inactivated fetal calf serum (Gibco BRL), 2 mmol/L glutamine and 50 μg/ml penicillin-streptomycin, at 37°C in a humidified atmosphere containing 5% carbon dioxide.

Immunohistochemical Studies

MCL tumors were analyzed immunohistochemically using a rabbit polyclonal antibody anti-survivin directed against the full-length recombinant survivin (Novus Biologicals, Littleton, CO), a mouse monoclonal anti-Ki-67 (Immunotech, Marseille, France) and a rabbit polyclonal antibody against cleaved caspase-3, which only recognizes the large fragment of caspase-3 that results after cleavage of procaspase-3 at Asp175 position (Cell Signaling, Beverly, MA). Antigen retrieval conditions and antibody dilutions are shown in Table 1. Briefly, paraffin sections on silane-coated slides were dewaxed and then subjected to antigen retrieval using a hot start method with the adequate buffer solution in a pressure cooker for 2 to 5 minutes at highest pressure, depending on the antibody used (Table 1). Slides were stained using an automated immunostainer TechMate 500 Plus (DAKO, Carpinteria, CA) and the Envision System (DAKO), counterstained in Gill's hematoxylin and mounted in Pertex (Histolab GmbH, Göteborg, Germany).

Simultaneous demonstration of Ki-67 or cleaved caspase-3 and survivin expression was determined in 20 tumor samples using an Universal DAKO Envision Doublestain System (DAKO) following the supplier instructions. Briefly, a unique common retrieval treatment was made for double staining of Ki-67 and survivin, but for double staining of cleaved caspase-3 and survivin, samples were subjected to pressure cooker in adequate buffer before each primary antibody incubation. Survivin immunostaining was performed using the DAB-peroxidase Envision method. After washing, slides were re-incubated with either anti-Ki-67 or anti-cleaved caspase-3 and then an APAAP-Envision method was used.

Immunohistochemical results were expressed as percentage of positive cells. A minimum of 1000 cells per case was counted in representative areas of the tumor. Entrapped and involved follicular germinal centers were excluded for quantification.

RT-PCR Analysis

Total RNA was isolated from each frozen tumor sample and from cell lines using guanidinium thiocyanate method (Ultraspec; Biotecx Laboratories, Houston, TX). RNA was treated with DNase (Ambion, Austin, TX) to eliminate contaminating DNA. For cDNA synthesis, 1 μg of RNA and Taqman Reverse Transcriptions reagents (including Multiscribe reverse transcriptase and random hexamers) were used, as described by the manufacturer (Applied Biosystems, Foster City, CA). The primers and probe used to amplify and quantify survivin cDNA by real-time were designed using Primer Express software (Applied Biosystems) and were as follows: survivin F, 5′-ATT TGA ATC GCG GGA CCC-3′; survivin R, 5′-GAG AAA GGG CTG CCA GGC-3′ and survivin probe, FAM-5′-CAT GGG TGC CCC GAC GTT GC-3′-TAMRA. The primers and the probe were located in a region with no homology to the EPR-1 gene. Real-time monitoring of PCR amplification of cDNAs was done with Taqman Universal master mix (Applied Biosystems) using 200 nmol/L of probe and 100 nmol/L of each survivin primer, in the ABI Prism 7700 sequence Detection System (Applied Biosystems). Relative quantification of gene expression was performed as described in the Taqman user's manual using human β-glucoronidase (GUSB)(Applied Biosystems) as an internal control.

To examine separately the three splice variants of survivin mRNA, the same forward primer but different reverse primers were used, as described previously.[25] Amplification was performed in a total volume of 25 μl in the presence of 3 mmol/L $MgCl_2$, 0.5 μmol/L of each primer and 2.5 μl of each cDNA. RT-PCR amplification was performed with an initial denaturation step of 10 minutes at 95°C, followed by 40 cycles of 30 seconds at 95°C, 30 seconds annealing at 60°C, and 30 seconds elongation at 72°C.

DNA Ploidy

DNA ploidy of the tumors was studied by flow cytometry in 27 cases in which suitable material was available. The analysis was performed on 50-μm-thick sections obtained from formalin-fixed, paraffin-embedded tissues as previously described[26] and analyzed with an Epics Profile II flow cytometer (Coulter Company, Hialeah, FL). Non-neoplastic cells in the section under study were used as the internal standard of the diploid channel.

Western Blot Analysis

Western blot analysis was performed on whole, cytoplasmic, and nuclear protein lysates. Cryostat frozen sections were lysed in ice-cold buffer containing 10 mmol/L N-2-hydroxyethylpiperazine-N-2-ethanesulphoric acid (HEPES) (pH 7.9), 10 mmol/L KCl, 1.5 mmol/L $MgCl_2$, 0.1% Nonidet P-40, 0.5 mmol/L dithiothreitol, 2 μg/ml leupeptin, 5 μg/ml aprotinin, and 0.5 mmol/L phenylmethylsulfonyl fluoride for 15 minutes. After centrifugation at 3500 rpm, the supernatant was collected (cytosolic fraction) and the nuclear fraction was obtained by lysis of the precipitated nuclei in a buffer containing 80 mmol/L Tris-HCl (pH 6.8), 2% sodium dodecyl sulfate, 10% glycerol and 0.1 mol/L DTT. Total extracts were obtained by lysis of cryostat sections in the latter buffer. Fifty μg of protein were separated by electrophoresis on 12% polyacrylamide gel and transferred to Immobilon-P (Millipore, Bedford, MA) membranes. The membranes were incubated with a polyclonal antibody against survivin. This antibody was the same used in the immunohistochemical studies. Antibody binding was detected using a secondary antibody conjugated to horseradish peroxidase and an enhanced chemiluminescence (ECL) detection kit (Amersham, Buckinghamshire, UK). Equal protein loading was confirmed with α-tubulin antibody (Oncogene Science, Inc, Cambridge, MA).

Statistical Analysis

The Fisher's exact, χ^2, *t*-test and analysis of variance tests were used to analyze the association between the clinico-biological parameters and the following categorized variables: immunohistochemical survivin protein expression (cutpoint 20%), survivin mRNA expression by real-time RT-PCR (cutpoint, 2), Ki-67 (cutpoint 50%), and cleaved caspase 3 (cutpoint 0.8%). Testing and estimation of possible cutoff values for survivin and Ki-67 expression was done by maximally selected log-rank statistics. Correlation between survivin, Ki-67 and cleaved caspase-3 was ascertained by means of linear regression. Survival time was measured from the time the sample was obtained. Probability of survival was calculated by the method of Kaplan and Meier, and curves were compared by means of the log-rank test. All statistical tests were two-sided and the significance level was established at 0.05. All significant prognostic variables in the univariate study, as well as survivin expression, proliferative index and Ki-67 expression, were considered for multivariate analysis performed by the stepwise proportional hazard regression method of Cox (survival). All statistical tests were performed with the SPSS v10.06 statistical package (SPSS Inc., Chicago, IL).

Results

Analysis of Survivin Expression by Western Blot

Survivin expression was first studied in nuclear and cytoplasmic protein lysates from Granta 519, Raji, and Daudi human lymphoma cell lines. Western blot analysis using a polyclonal antibody directed against full-length recombinant survivin showed a dominant band of approximately 16.5 kd that was only observed in nuclear extracts from all of the cell lines tested (Figure 1A). In

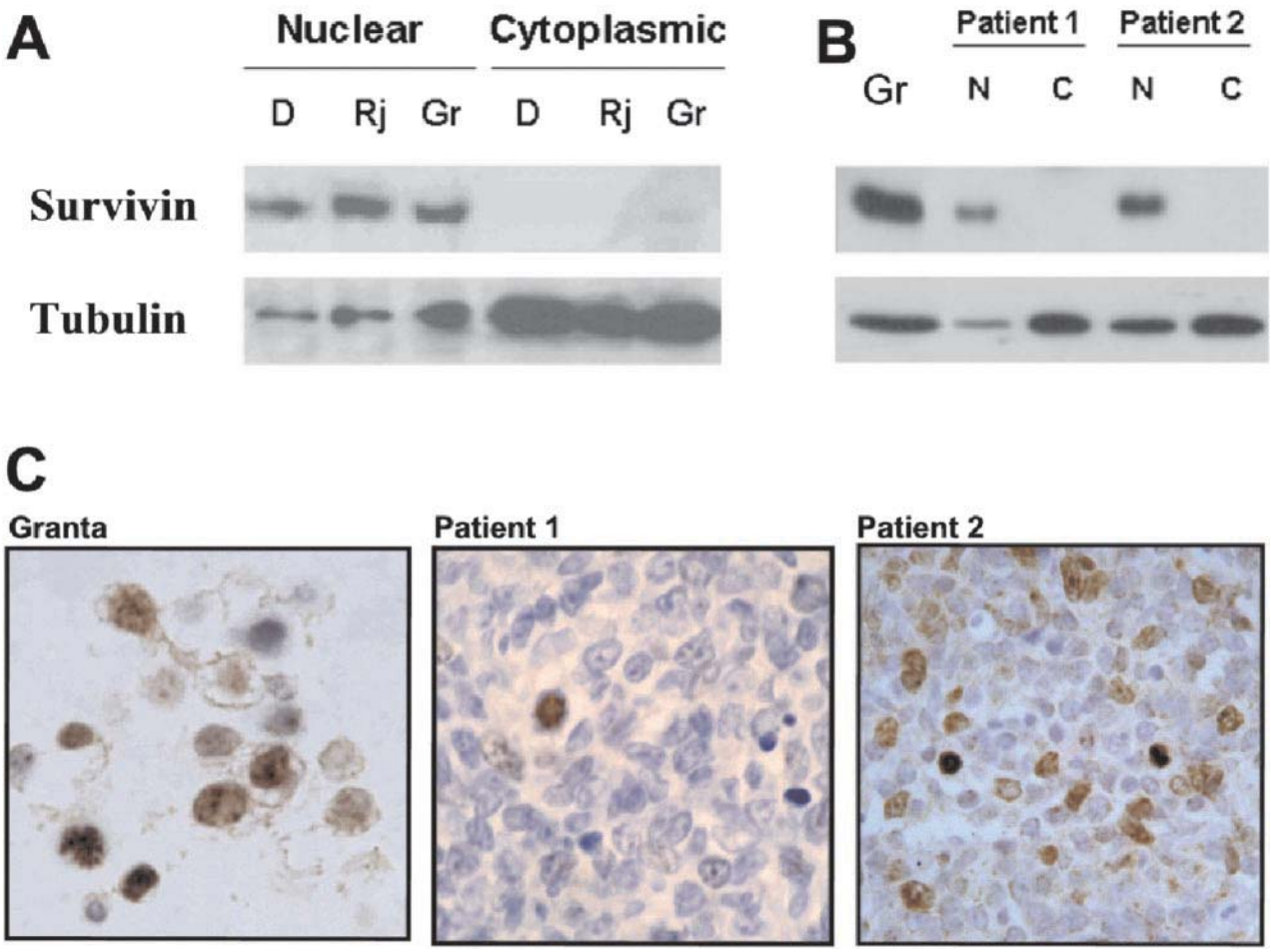

Figure 1. Western Blot analysis of survivin protein (Rj) in nuclear and cytoplasmic cell lysates from B human lymphoma cells and MCL patients. Nuclear and cytoplasmic protein lysates from Daudi (D), Raji (R) and Granta 519 (Gr) human cell lines (**A**) and from two representative MCL patients (**B**) were obtained and survivin expression was analyzed by Western blot. Expression of α-tubulin was used as a loading control. **C:** Immunostaining for survivin in cells from Granta 519 cell line and two representative MCL patients confirm the nuclear localization of survivin.

MCL tumors, survivin was also only detected in nuclear protein lysates (Figure 1B).

Analysis of Survivin Expression by Immunohistochemistry

The nuclear expression of survivin observed by Western blot was confirmed by immunohistochemistry in all of the cell lines tested and MCL tumors (Figure 1C). Some cells showed weak cytoplasmic staining that tended to disappear with progressive antibody dilutions (data not shown). In reactive lymph nodes and adult tonsils, survivin-positive cells were found mainly in the nucleus of proliferating germinal center cells, and only scattered cells in the mantle zone were positive (Figure 2A). To further confirm this nuclear localization in other lymphoid tumors, additional immunohistochemical studies were performed in a short series of diffuse large B-cell lymphomas (DLBCL) and chronic lymphocytic leukemia (CLL). In all cases, survivin staining was exclusively nuclear as in MCL cases.

Survivin expression was examined immunohistochemically in 80 MCL. A variable number of survivin nuclear-positive cells ranging from 5% to 95% was detected (Figure 2, B to D). This nuclear distribution of survivin was homogeneous with nucleolar enhancement in non-mitotic nuclei and more intense and granular in prophase (Figure 3A). In metaphase, anaphase, and telophase chromosomes were strongly stained, whereas mitotic spindles were also occasionally observed with a weaker labeling (Figure 3B). Survivin-positive cells were diffusely distributed throughout the tumor. However, in some cases, reactive and colonized germinal centers were easily recognized as nodular clusters of cells with strong survivin nuclear positivity (Figure 2B). Colonization of germinal centers by tumor cells was confirmed by detection of numerous cyclin D1-positive cells within the germinal centers.

The number of survivin-positive cells correlated with the histological subtype of MCL. Thus, the highest expression of survivin was observed in the blastic variant (30 ± 29% of positive cells, $n = 14$), compared to classical MCL (10 ± 10%, $n = 57$) (analysis of variance, $P < 0.0001$). The expression of survivin in pleomorphic MCL was similar to that observed in classical tumors (10 ± 12%, $n = 9$; $P = 0.89$) (Figure 4).

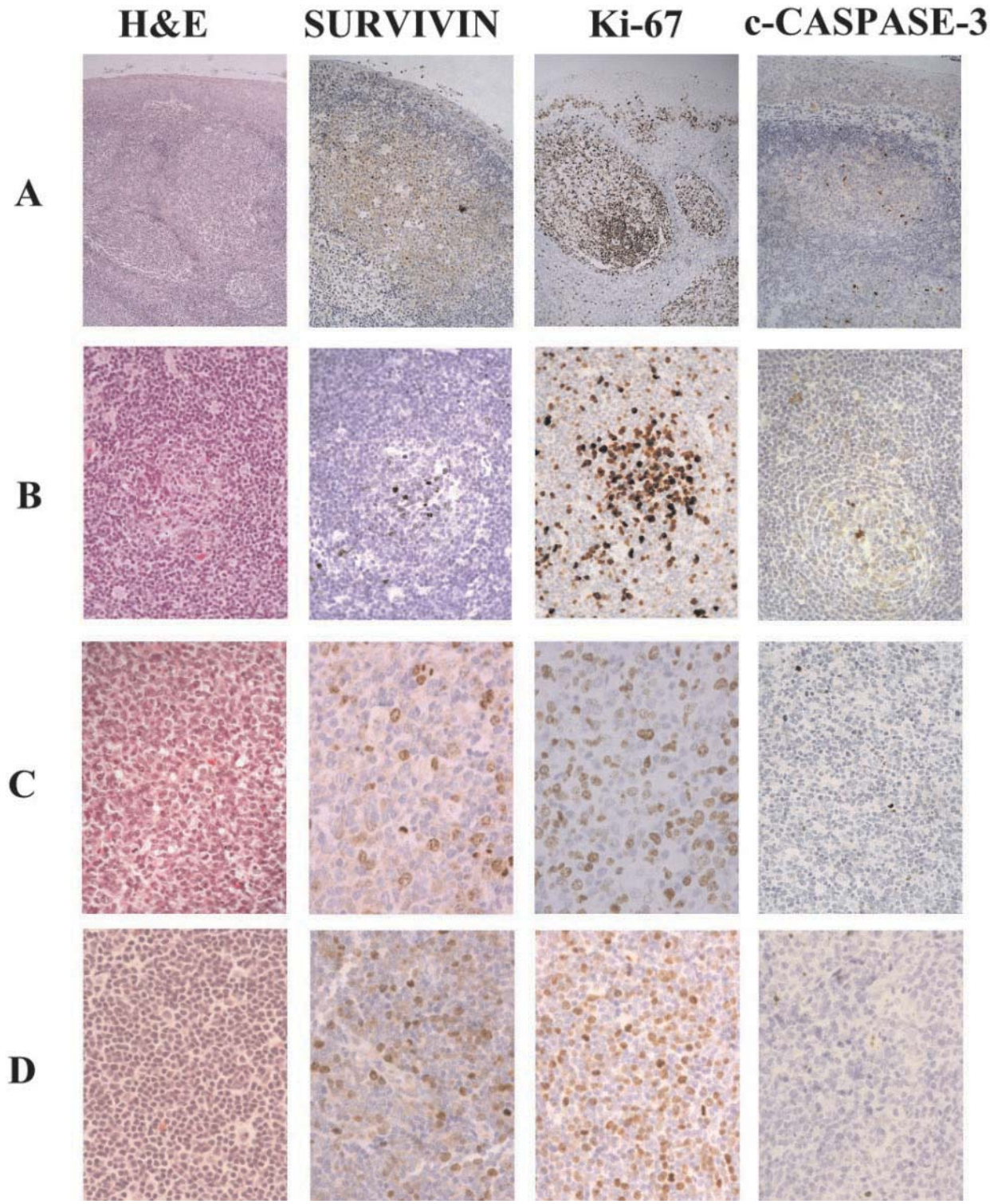

Figure 2. Survivin, Ki-67, and cleaved caspase-3 expression in reactive tonsil and MCL. **A:** Adult tonsil. Reactive tonsil showing a number of hyperplastic follicles (hematoxylin and eosin, H&E). Cells expressing survivin, Ki-67, and cleaved caspase-3 were mainly localized in the germinal center of secondary follicles. **B:** MCL, classical variant. An entrapped reactive germinal center was colonized by tumor cells (H&E). Cyclin D1 staining confirmed the presence of tumor cells inside the reactive germinal center (not shown). Survivin-positive tumor and reactive cells were clustered in a partially involved germinal center. Only very few scattered cells were positive outside the follicle. The proliferative activity of the tumor was low. A very low number of positive cleaved caspase-3 cells were detected in the tumor. Apoptotic activity was mostly concentrated in the entrapped follicles. **C:** MCL, pleomorphic variant. A high mitotic activity was observed in this tumor (H&E). Survivin-positive cells were widely distributed through the tumor. A high number of Ki-67 positive cells were also detected. A few cells were positive for cleaved caspase-3. **D:** MCL, blastic variant. Monotonous infiltration by medium-sized lymphocytes with rounded nuclei and dispersed chromatin (H&E). Survivin was widely expressed in tumor cells. Increased proliferative activity was noticed with Ki-67 antigen. A few number of cells were positive for cleaved caspase-3. Original magnification, ×200

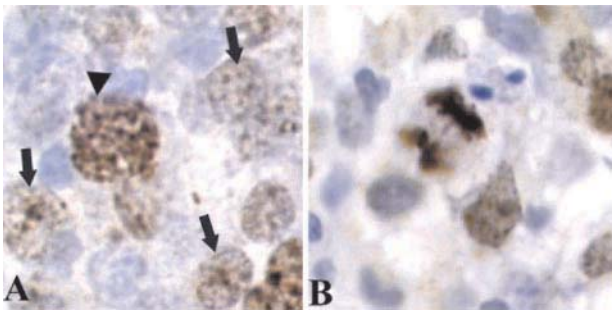

Figure 3. Nuclear and mitotic pattern of survivin expression in primary MCL cells. **A:** Survivin expression showed a homogeneous pattern with nucleolar reinforcement in non-mitotic nuclei (**arrows**) and a strong multi-granular pattern in large-sized prophasic appearing nuclei (**arrowheads**). **B:** In late mitotic nuclei, chromosomes were strongly stained. Original magnification, ×1000

No changes in survivin levels were observed in 10 paired samples of five classical MCL at different times of disease, without evidence of tumor progression (11 ± 9% *vs.* 13 ± 8%). In two additional patients who had progressed from classical to blastoid MCL, an increase in the number of survivin-positive cells was observed in the blastoid variant (1.4- and three-fold, respectively).

Analysis of Survivin Expression by Real-Time RT-PCR

Quantification of survivin expression was assessed by real-time RT-PCR. The comparative C_T (cycle threshold) method was used for relative quantification of survivin mRNA expression, after confirming that survivin cDNA and GUS cDNA were amplified with the same efficiency. Survivin expression in normal lymphocytes was used as a reference control, and the survivin expression levels of these cells adopted the arbitrary value of 1. Granta 519, a MCL-derived cell line, showed 100-fold increase in survivin levels compared to normal lymphocytes. The expression of survivin by real-time RT-PCR was analyzed in 51 MCL tumors. Survivin mRNA was detected in all MCL samples, with a mean relative value of 4 ± 4. Higher levels of survivin mRNA were detected in the blastic MCL variants (10 ± 7, $n = 7$), compared to those obtained in classical (4 ± 3, $n = 41$) and pleomorphic (3 ± 2, $n = 3$) tumors (Figure 5). Moreover, a significant linear correlation was found between mRNA survivin levels and the number of survivin-positive cells analyzed by immunohistochemistry (Pearson Regression Test, $P < 0.0001$).

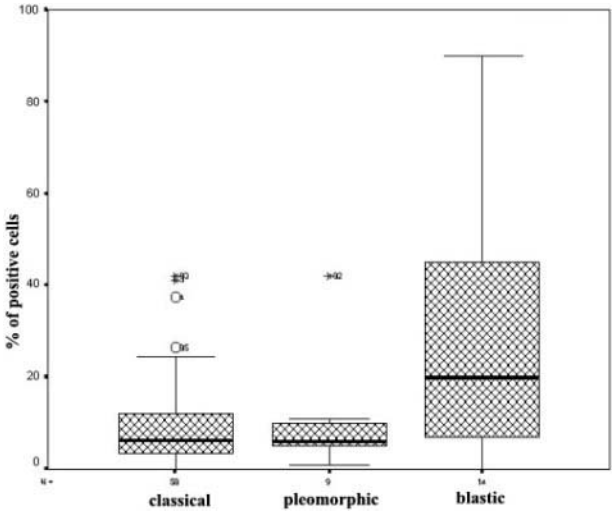

Figure 4. Immunohistochemical analysis of survivin expression in MCL. Blastic MCL variant showed higher survivin expression than classical and pleomorphic MCL variants. Symbols above the bars represent outlier cases.

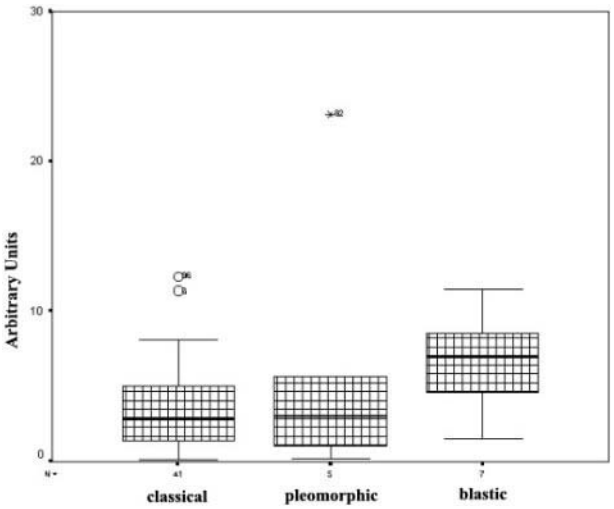

Figure 5. Real-time RT-PCR quantitative analysis of survivin mRNA expression in MCL. Blastic MCL variant showed higher survivin mRNA expression than classical and pleomorphic MCL variants. Survivin mRNA expression levels are given in arbitrary units using normal lymphocytes as reference control. PCR arbitrary units were defined as described in Material and Methods. Symbols above the bars represent outlier cases.

Analysis of Survivin Variants by RT-PCR

Using specific primers, the different survivin variants were detected in seven MCL tumors. The specificity of amplification products was confirmed by DNA sequencing (data not shown). In all MCL cases, survivin, survivin-2B and survivin-ΔEx3 mRNA were detected. A series of six DLBCL and five CLL cases were also analyzed. The three survivin variants were detected in all DLBCL, with an expression pattern similar to MCL samples. The expression pattern of these splicing variants was heterogeneous in the CLL patients since survivin was detected in four patients, survivin-2B in two and survivin-ΔEx3 only in one of the five patients.

Correlation of Survivin Expression with Cell Proliferation, Apoptosis, and Ploidy Status in MCL

Survivin expression was compared to the proliferative activity and apoptotic index of the tumors. The proliferative activity was analyzed in 82 MCL tumors and it was calculated as the percentage of Ki-67 positive cells in the most proliferative areas, excluding colonized follicles. The apoptotic index was calculated in 55 cases as the

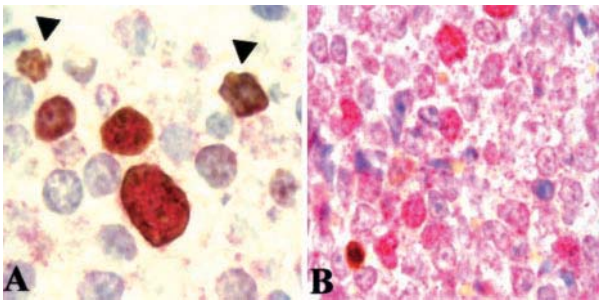

Figure 6. Double immunohistochemical staining of survivin and Ki-67 or cleaved caspase-3. **A:** Survivin/Ki-67 staining. All survivin-positive cells (red) were also Ki-67-positive cells (brown) (×60). Some cells were only positive for Ki-67 (**arrows**). **B:** Survivin/cleaved caspase-3 staining. A wide number of tumor cells were positive for survivin expression (red) but only few cells were stained with the antibody against cleaved caspase-3 (brown). No double-positive cells were found. Original magnification, ×1000.

percentage of positive cells stained with anti-cleaved caspase-3, the active form of caspase-3.

Blastic MCL cases showed a higher proliferative index (63 ± 29%, $n = 14$) than classical (30 ± 23%, $n = 57$) (analysis of variance, $P < 0001$) or pleomorphic (40 ± 29%, $n = 9$) MCL variants (Figure 2, B to D). The proliferative activity of the tumors showed a statistically significant correlation with protein and mRNA survivin expression levels measured by immunohistochemistry (Pearson Regression Test, $P = 0.001$) or real-time quantitative RT-PCR (Pearson Regression Test, $P = 0.0001$), respectively.

Double immunolabeling for Ki-67 and survivin was performed in 20 selected tumors. In all cases, a nuclear co-localization of both proteins was observed, although the number of Ki-67 positive cells was higher than survivin stained cells. Of note, virtually all cells positive for survivin also expressed the Ki-67 antigen (Figure 6A).

In all MCL cases, the number of cells labeled with anti-cleaved caspase-3 was low, ranging from 0.1% to 5.6% (Figure 2). In all of the samples analyzed, the areas showing the highest positivity for cleaved caspase-3 were also the most proliferative areas (data not shown). Although a higher apoptotic activity was observed in blastic and pleomorphic variants, no significant differences in cleaved caspase-3 expression among the histological subtypes were found. Moreover, no correlation between survivin expression and the apoptosis index was observed. Using a double-immunohistochemical labeling for cleaved caspase-3 and survivin, no cells simultaneously positive for both antigens were identified (Figure 6B).

In 27 cases, the ploidy status was assessed by flow cytometry. Tetraploidy was found in 5 of 6 pleomorphic MCL (83%), in 2 of 6 blastic variant (33%) and only in 2 of 15 classical tumors (13%) (χ^2, $P = 0.03$). By immunohistochemistry, no differences in survivin levels were observed between diploid (17 ± 16%) and tetraploid (16 ± 16%) MCL cases.

Prognostic Significance of Survivin Expression

The main clinical characteristics and follow-up were available in 62 patients. Median follow-up of the series

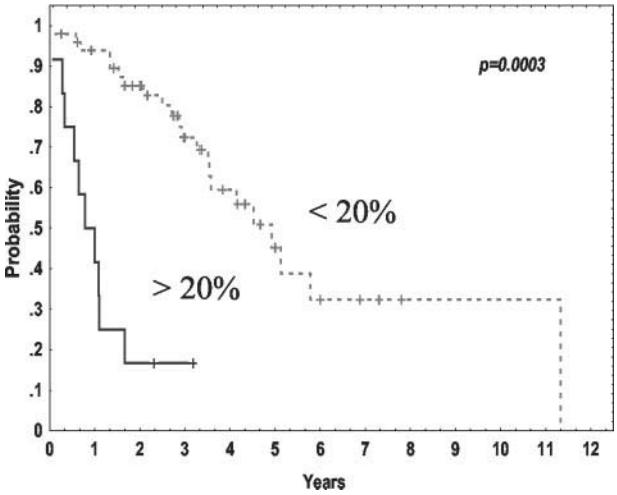

Figure 7. Overall survival of 62 MCL patients according to survivin protein expression analyzed by immunohistochemistry.

was 36 months. Among the clinical features at diagnosis, mRNA survivin expression correlated only with the performance status of the patients (ECOG ≥2, χ^2, $P = 0.05$). No relationship between survivin levels and other clinicobiological parameters was found. Moreover, no correlation of survivin levels with the degree of therapeutical response was detected. Interestingly, increased survivin expression assessed by both real-time RT-PCR and immunohistochemistry correlated with a shorter survival of the patients. Thus, patients with survivin expression in more than 20% of tumor cells had a median survival of 8 months, whereas it was of 60 months for those patients with survivin staining in ≤20% (Kaplan-Meier, log survival $P = 0.0003$) (Figure 7). Furthermore, the median survival of the patients with high and low survivin mRNA expression was 24 and 80 months, respectively (Kaplan-Meier, log survival $P = 0.00023$).

Ki-67 expression was also able to predict survival in MCL patients. Patients with Ki-67 expression in more than 50% of tumor cells had a median survival of 9 months, whereas it was 62 months for patients with less than 50% of Ki-67-positive cells (Kaplan-Meier, log survival $P =$ 0,0006). Furthermore, Ki-67 expression was able to predict survival in typical histological variants ($P = 0.022$), but did not predict survival in either the blastic or pleomorphic variants. This was probably due to the fact that virtually all blastic variants (8 of 10) exhibited high Ki-67 expression. When Ki-67 expression (considering 50% cut-off) was compared to the histological variants (typical *versus* blastoid) in a multivariate analysis for survival, only the Ki-67 expression remained into the model (Cox Multivariate Test, risk ratio (RR) = 4.4; 0.95 CI of RR = 1.9 to 9.9). In addition, in a Cox multivariate analysis comparing survivin *versus* the proliferative index for survival, Ki-67 expression, but not the survivin levels, retained its prognostic value (RR = 10.88; $P = 0.0001$).

Discussion

In this study, we have examined survivin expression in a large series of MCL and the results have been compared

to different pathological characteristics of the tumors and clinical parameters of the patients. Our findings indicate that survivin is commonly expressed in these tumors with a nuclear and mitotic pattern. The expression levels were significantly associated with the histological variants and proliferative activity of the tumors as well as with the survival of the patients. However, survivin levels were not related to the ploidy or caspase-3 activation in these tumors.

Survivin was only detected in the nuclear fraction of tumor cells. In mitotic cells, after nuclear membrane disruption, survivin strongly labeled chromosomes and the mitotic spindle. These immunohistochemical observations were also confirmed by Western blot analysis showing survivin expression mainly in the nuclear but not in the cytoplasmic fraction of cell lysates. A similar nuclear staining was also observed in normal lymphocytes of reactive germinal centers. These staining patterns in a human lymphoid neoplasm are concordant with previous observations in human cancer cell lines in which survivin has been associated with centromeres, mitotic spindle microtubules, centrosomes, and cytokinesis.[16,27–30] Previous studies analyzing survivin expression by immunohistochemistry have shown a predominant cytoplasmic distribution.[15,31] However, nuclear accumulation of survivin has been recently described in other human tumors.[32,33] The reason for these differences in cell distribution between tumors is not clear. It has been proposed that the subcellular distribution of survivin is regulated by an active import into the nucleus and a CRM1-mediated export to the cytoplasm, suggesting that survivin may be considered a nuclear shuttling protein. Therefore, the almost exclusively cytoplasmic localization in a high number of tumors may be the result of a higher rate of nuclear export.[34]

Survivin expression was detected in all tumors with a variable number of positive cells ranging from 5% to 95%. The number of positive cells detected by immunohistochemistry correlated significantly with the mRNA levels detected by real-time quantitative RT-PCR ($P < 0.0001$), suggesting that survivin expression in these tumors is predominantly regulated at the transcriptional level. The survivin gene gives three alternatively spliced transcripts. In addition to wild-type survivin, which exhibits a three-intron-four exon structure, two survivin isoforms were generated by insertion of an alternative exon 2 (survivin-2B) or removal of exon 3 (survivin-ΔEx3).[25] In MCL cases the three survivin variants were detected.

Higher levels of survivin were detected in blastic MCL than in classic or pleomorphic variants. In addition, survivin expression levels were significantly associated with the proliferative activity of the tumors. Blastic variant of MCL has a higher proliferative activity and a more aggressive biological behavior than classical forms of this tumor.[35] Concordantly, MCL patients with high survivin expression had a shorter overall survival. In this regard, it is of note that survivin overexpression in other human cancers has been associated with unfavorable prognostic features, poor response to therapy, high relapse rate and shortened survival.[17–20] Furthermore, survivin has been considered an independent prognostic factor in DLBL.[36] However, the multivariate analysis performed in our study indicates that survival in MCL was better predicted by the proliferative activity of the tumors than by survivin levels. This finding is concordant with previous studies indicating that proliferation is one of the best prognosis parameters in MCL.[35,37] The relationship between survivin expression, proliferation, and survival in other human tumors has not been explored. Recently, it has been described that in CLL cells, survivin is the only IAP whose expression is induced by CD40L, suggesting a role of survivin in the control of CLL proliferative pool interfacing apoptosis.[38] The protective anti-apoptotic effect of survivin in proliferating malignant cells may be a mechanism to stabilize tumor cells with chromosomal abnormalities favoring the survival of these cells and the progression of the tumors.[29]

Survivin seems to be required for the targeting of members of the Aurora family of kinases to metaphase chromosomes, thereby controlling chromosome segregation and possibly cytokenesis.[28,29,39] Recently, it has been described that the preponderant survivin pool is associated with microtubules and participates in the assembly of a bipolar mitotic spindle.[40] This function is consistent with its localization to centrosomes, spindle pores, and spindle microtubules.[16,40] Furthermore, suppression of human survivin expression induces a catastrophic defect of microtubule assembly, with abnormal mitotic spindles and formation of multinucleated cells.[27,29,41,42] MCL is characterized by an increased number of chromosomal imbalances and ploidy alterations.[7–9] In addition, tetraploidy is a common numerical chromosomal aberration in blastic and pleomorphic MCL variants.[10] In this sense, we found tetraploidy in 83% of pleomorphic MCL and in 33% of blastic tumors but only in 13% of classical variants. However, no differences in survivin levels were detected in MCL in correlation with the ploidy status, suggesting that survivin expression may not be involved in the generation of this type of chromosomal aberrations.

Survivin has been implicated in a dual role connecting suppression of apoptosis to regulation of chromosomal segregation and cell division.[16,19] Targeting experiments using antisense survivin or dominant-negative mutants resulted in spontaneous apoptosis, increased caspase activity, and inhibition of cell proliferation.[26,40,42] A role for survivin in blocking apoptosis has also been demonstrated *in vivo*.[43] However, the mechanisms of apoptotic suppression by survivin are not completely clear. Initial observations suggested that survivin could directly suppress activation of caspase-3[44,45]; however, more recent studies have demonstrated that survivin lacks the ability to directly inhibit caspase-3.[46,47] Other groups have proposed that survivin acts like other IAPs by binding to caspase-9 and/or by neutralizing the new IAP-inhibiting protein, Smac/Diablo,[48,49] raising the possibility that it might suppress caspases indirectly by freeing other IAP family members from the constraints of this protein. In this study we have investigated the apoptotic activity in MCL by examining the expression of the cleaved form of caspase-3. This immunohistochemical assay has been recently used in other B cell lymphomas, showing that the number of apoptotic cells was variable in different types

of tumors.[50] However, in this study, MCL tumors were not examined. Our findings demonstrate that expression of cleaved caspase-3 in MCL was virtually absent or very low in most tumors. Furthermore, survivin and cleaved caspase-3 were never expressed in the same MCL cell. This low percentage of apoptotic cells and the detection of survivin in MCL are in agreement with a potential role of survivin in inhibiting apoptosis.

In conclusion, our results indicate that survivin is commonly expressed in MCL with a nuclear and mitotic pattern and that its expression levels are strongly associated with the proliferative activity of the tumors and the survival of the patients, suggesting a potential role in cell cycle regulation and tumor progression. The dual role of survivin in apoptosis inhibition and regulation of cell cycle may facilitate evasion from checkpoint mechanisms of growth arrest and promote resistance to chemotherapeutic regimens targeting the mitotic spindle. Since MCL cells showed alterations in cell cycle regulator genes as well as a poor response to conventional treatments, manipulation of survivin expression might be of interest in the treatment of MCL.

Acknowledgments

We thank Montse Sanchez for the excellent technical assistance. Montse Sanchez was supported by Dako.

References

1. Campo E, Raffeld M, Jaffe ES: Mantle-cell lymphoma. Semin Hematol 1999, 36:115–127
2. Bosch F, Jares P, Campo E, Lopez-Guillermo A, Piris MA, Villamor N, Tassies D, Jaffe ES, Montserrat E, Rozman C, Cardesa A: PRAD-1/cyclin D1 gene overexpression in chronic lymphoproliferative disorders: a highly specific marker of mantle cell lymphoma. Blood 1994, 84:2726–2732
3. Hernandez L, Fest T, Cazorla M, Teruya-Feldstein J, Bosch F, Peinado MA, Piris MA, Montserrat E, Cardesa A, Jaffe ES, Campo E, Raffeld M: p53 gene mutations and protein overexpression are associated with aggressive variants of mantle cell lymphomas. Blood 1996, 87:3351–3359
4. Greiner TC, Moynihan MJ, Chan WC, Lytle DM, Pedersen A, Anderson JR, Weisenburger DD: p53 mutations in mantle cell lymphoma are associated with variant cytology and predict a poor prognosis. Blood 1996, 87:4302–4310
5. Pinyol M, Hernandez L, Cazorla M, Balbín M, Jares P, Fernández PL, Montserrat E, Cardesa A, Lopez-Otin C, Campo E: Deletions and loss of expression of p16INK4a and p21Waf1 genes are associated with aggressive variants of mantle cell lymphomas. Blood 1997, 89:272–280
6. Dreyling MH, Bullinger L, Ott G, Stilgenbauer S, Muller-Hermelink HK, Bentz M, Hiddemann W, Dohner H: Alterations of the cyclin D1/p16-pRB pathway in mantle cell lymphoma. Cancer Res 1997, 57:4608–4614
7. Bea S, Ribas M, Hernandez JM, Bosch F, Pinyol M, Hernandez L, Garcia JL, Flores T, Gonzalez M, Lopez-Guillermo A, Piris MA, Cardesa A, Montserrat E, Miro R, Campo E: Increased number of chromosomal imbalances and high-level DNA amplifications in mantle cell lymphoma are associated with blastoid variants. Blood 1999, 93:4365–4374
8. Bentz M, Plesch A, Bullinger L, Stilgenbauer S, Ott G, Muller-Hermelink HK, Baudis M, Barth TF, Moller P, Lichter P, Dohner H: t(11;14)-positive mantle cell lymphomas exhibit complex karyotypes and share similarities with B-cell chronic lymphocytic leukemia. Genes Chromosomes Cancer 2000, 27:285–294
9. Allen JE, Hough RE, Goepel JR, Bottomley S, Wilson GA, Alcock HE, Baird M, Lorigan PC, Vandenberghe EA, Hancock BW, Hammond DW: Identification of novel regions of amplification and deletion within mantle cell lymphoma DNA by comparative genomic hybridization. Br J Haematol 2002, 116:291–298
10. Ott G, Kalla J, Ott MM, Schryen B, Katzenberger T, Muller JG, Muller-Hermelink HK: Blastoid variants of mantle cell lymphoma: frequent bcl-1 rearrangements at the major translocation cluster region and tetraploid chromosome clones. Blood 1997, 89:1421–1429
11. Camacho E, Hernandez L, Hernandez S, Tort F, Bellosillo B, Bea S, Bosch F, Montserrat E, Cardesa A, Fernández PL, Campo E: ATM gene inactivation in mantle cell lymphoma mainly occurs by truncating mutations and missense mutations involving the phosphatidylinositol-3 kinase domain and is associated with increasing numbers of chromosomal imbalances. Blood 2002, 99:238–244
12. Tort F, Hernandez S, Bea S, Martinez A, Esteller M, Herman JG, Puig X, Camacho E, Hernández L, Sanchez M, Nayach I, Lopez-Guillermo A, Fernández PL, Colomer D, Campo E: CHK2-decreased protein expression and infrequent genetic alterations mainly occur in aggressive types of non-Hodgkin's lymphomas. Blood 2002, 100:4602–4608
13. Reed JC: Apoptosis-based therapies. Nat Rev Drug Discov 2002, 1:111–121
14. Deveraux QL, Reed JC: IAP family proteins-suppressors of apoptosis. Genes Dev 1999, 13:239–252
15. Ambrosini G, Adida C, Altieri DC: A novel anti-apoptosis gene, survivin, expressed in cancer and lymphoma. Nat Med 1997, 3:917–921
16. Li F, Ambrosini G, Chu EY, Plescia J, Tognin S, Marchisio PC, Altieri DC: Control of apoptosis and mitotic spindle checkpoint by survivin. Nature 1998, 396:580–584
17. Kawasaki H, Altieri DC, Lu CD, Toyoda M, Tenjo T, Tanigawa N: Inhibition of apoptosis by survivin predicts shorter survival rates in colorectal cancer. Cancer Res 1998, 58:5071–5074
18. Islam A, Kageyama H, Takada N, Kawamoto T, Takayasu H, Isogai E, Ohira M, Hashizume K, Kobayashi H, Kaneko Y, Nakagawara A: High expression of Survivin, mapped to 17q25, is significantly associated with poor prognostic factors and promotes cell survival in human neuroblastoma. Oncogene 2000, 19:617–623
19. Altieri DC: The molecular basis and potential role of survivin in cancer diagnosis and therapy. Trends Mol Med 2001, 7:542–547
20. Ikeguchi M, Ueda T, Sakatani T, Hirooka Y, Kaibara N: Expression of survivin messenger RNA correlates with poor prognosis in patients with hepatocellular carcinoma. Diagn Mol Pathol 2002, 11:33–40
21. Kallio MJ, Nieminen M, Eriksson JE: Human inhibitor of apoptosis protein (IAP) survivin participates in regulation of chromosome segregation and mitotic exit. EMBO J 2001, 15:2721–2723
22. Bolton MA, Lan W, Powers SE, McCleland ML, Kuang J, Stukenberg PT: Aurora B kinase exists in a complex with survivin and INCENP and its kinase activity is stimulated by survivin binding and phosphorylation. Mol Biol Cell 2002, 13:3064–3077
23. Jaffe ES, Harris NL, Stein H, Vardiman JWE: World Health Organization classification of tumors. Pathology and Genetics of Tumours of Haematopoietic and Lymphoid Tissues. Edited by ES Jaffe, NL Harris, H Stein, JWE Vardiman. Lyon, France: IARC Press, 2001, pp 168–170
24. A predictive model for aggressive non-Hodgkin's lymphoma. The International Non-Hodgkin's Lymphoma Prognostic Factors Project. N Engl J Med 1993, 329:987–994
25. Mahotka C, Krieg T, Krieg A, Wenzel M, Suschek CV, Heydthausen M, Gabbert HE, Gerharz CD: Distinct in vivo expression patterns of survivin splice variants in renal cell carcinomas. Int J Cancer 2002, 100:30–36
26. Hedley DW, Friedlander ML, Taylor IW, Rugg CA, Musgrove EA: Method for analysis of cellular DNA content of paraffin-embedded pathological material using flow cytometry. J Histochem Cytochem 1983, 31:1333–1335
27. Li F, Ackermann EJ, Bennett CF, Rothermel AL, Plescia J, Tognin S, Villa A, Marchisio PC, Altieri DC: Pleiotropic cell-division defects and apoptosis induced by interference with survivin function. Nat Cell Biol 1999, 1:461–466
28. Skoufias DA, Mollinari C, Lacroix FB, Margolis RL: Human survivin is a kinetochore-associated passenger protein. J Cell Biol 2000, 151:1575–1582
29. Uren AG, Wong L, Pakusch M, Fowler KJ, Burrows FJ, Vaux DL, Choo KH: Survivin and the inner centromere protein INCENP show similar

cell-cycle localization and gene knockout phenotype. Curr Biol 2000, 10:1319–1328
30. Giodini A, Kallio MJ, Wall NR, Gorbsky GJ, Tognin S, Marchisio PC, Symons M, Altieri DC: Regulation of microtubule stability and mitotic progression by survivin. Cancer Res 2002, 62:2462–2467
31. Adida C, Recher C, Raffoux E, Daniel MT, Taksin AL, Rousselot P, Sigaux F, Degos L, Altieri DC, Dombret H: Expression and prognostic significance of survivin in de novo acute myeloid leukaemia. Br J Haematol 2000, 111:196–203
32. Okada E, Murai Y, Matsui K, Isizawa S, Cheng C, Masuda M, Tacaño Y: Survivin expression in tumor cell nuclei is predictive of a favorable prognosis in gastric cancer patients. Cancer Lett 2001, 163:109–116
33. Frost M, Jarboe EA, Orlicky D, Gianani R, Thompson LC, Enomoto T, Shroyer KR: Immunohistochemical localization of survivin in benign cervical mucosa, cervical dysplasia, and invasive squamous cell carcinoma. Am J Clin Pathol 2002, 117:738–744
34. Rodriguez JA, Span SW, Ferreira CG, Kruyt FA, Giaccone G: CRM1-mediated nuclear export determines the cytoplasmic localization of the antiapoptotic protein survivin. Exp Cell Res 2002, 275:44–53
35. Bosch F, Lopez-Guillermo A, Campo E, Ribera JM, Conde E, Piris MA, Vallespi T, Woessner S, Montserrat E: Mantle cell lymphoma: presenting features, response to therapy, and prognostic factors. Cancer 1998, 82:567–575
36. Adida C, Haioun C, Gaulard P, Lepage E, Morel P, Briere J, Dombret H, Reyes F, Diebold J, Gisselbrecht C, Salles G, Altieri DC, Molina TJ: Prognostic significance of survivin expression in diffuse large B-cell lymphomas. Blood 2000, 96:1921–1925
37. Velders GA, Kluin-Nelemans JC, De Boer CJ, Hermans J, Noordijk EM, Schuuring E, Kramer MH, Van Deijk WA, Rahder JB, Kluin PM, Van Krieken JH: Mantle-cell lymphoma: a population-based clinical study. J Clin Oncol 1996, 14:1269–1274
38. Granziero L, Ghia P, Circosta P, Gottardi D, Strola G, Geuna M, Montagna L, Piccoli P, Chilosi M, Caligaris-Cappio F: Survivin is expressed on CD40 stimulation and interfaces proliferation and apoptosis in B-cell chronic lymphocytic leukemia. Blood 2001, 97:2777–2783
39. Wheatley SP, Carvalho A, Vagnarelli P, Earnshaw WC: INCENP is required for proper targeting of survivin to the centromeres and the anaphase spindle during mitosis. Curr Biol 2001, 11:886–890
49. Fortugno P, Wall NR, Giodini A, O'Connor DS, Plescia J, Padgett KM, Tognin S, Marchisio PC, Altieri DC: Survivin exists in immunochemically distinct subcellular pools and is involved in spindle microtubule function. J Cell Sci 2002, 115:575–585
41. Chen J, Wu W, Tahir SK, Kroeger PE, Rosenberg SH, Cowsert LM, Bennett F, Krajewski S, Krajewska M, Welsh K, Reed JC, Ng SC: Down-regulation of survivin by antisense oligonucleotides increases apoptosis, inhibits cytokinesis and anchorage-independent growth. Neoplasia 2000, 2:235–241
42. Olie RA, Simoes-Wust AP, Baumann B, Leech SH, Fabbro D, Stahel RA, Zangemeister-Wittke U: A novel antisense oligonucleotide targeting survivin expression induces apoptosis and sensitizes lung cancer cells to chemotherapy. Cancer Res 2000, 60:2805–2809
43. Grossman D, Kim PJ, Schechner JS, Altieri DC: Inhibition of melanoma tumor growth in vivo by survivin targeting. Proc Natl Acad Sci USA 2001, 98:635–640
44. Tamm I, Wang Y, Sausville E, Scudiero DA, Vigna N, Oltersdorf T, Reed JC: IAP-family protein survivin inhibits caspase activity and apoptosis induced by Fas (CD95), Bax, caspases, and anticancer drugs. Cancer Res 1998, 58:5315–5320
45. Suzuki A, Ito T, Kawano H, Hayashida M, Hayasaki Y, Tsutomi Y, Akahane K, Nakano T, Miura M, Shiraki K: Survivin initiates procaspase 3/p21 complex formation as a result of interaction with Cdk4 to resist Fas-mediated cell death. Oncogene 2000, 19:1346–1353
46. Verdecia MA, Huang H, Dutil E, Kaiser DA, Hunter T, Noel JP: Structure of the human anti-apoptotic protein survivin reveals a dimeric arrangement. Nat Struct Biol 2000, 7:602–608
47. Banks DP, Plescia J, Altieri DC, Chen J, Rosenberg SH, Zhang H, Ng SC: Survivin does not inhibit caspase-3 activity. Blood 2000, 96: 4002–4003
48. O'Connor DS, Grossman D, Plescia J, Li F, Zhang H, Villa A, Tognin S, Marchisio PC, Altieri DC: Regulation of apoptosis at cell division by p34cdc2 phosphorylation of survivin. Proc Natl Acad Sci USA 2000, 97:13103–1310
49. Du C, Fang M, Li Y, Li L, Wang X: Smac, a mitochondrial protein that promotes cytochrome c-dependent caspase activation by eliminating IAP inhibition. Cell 2000, 102:33–42
50. Dukers DF, Oudejans JJ, Vos W, ten Berge RL, Meijer CJ: Apoptosis in B-cell lymphomas and reactive lymphoid tissues always involves activation of caspase 3 as determined by a new in situ detection method. J Pathol 2002, 196:307–315

ORIGINAL ARTICLE

ZAP-70 Expression as a Surrogate for Immunoglobulin-Variable-Region Mutations in Chronic Lymphocytic Leukemia

Marta Crespo, B.S., Francesc Bosch, M.D., Neus Villamor, M.D., Beatriz Bellosillo, Ph.D., Dolors Colomer, Ph.D., María Rozman, M.D., Silvia Marcé, B.S., Armando López-Guillermo, M.D., Elies Campo, M.D., and Emili Montserrat, M.D.

ABSTRACT

BACKGROUND

The mutational status of immunoglobulin heavy-chain variable-region (IgV_H) genes in the leukemic cells of chronic lymphocytic leukemia (CLL) is an important prognostic factor in the disease. We investigated whether the expression of ZAP-70 by CLL cells correlated with the IgV_H mutational status, disease progression, and survival.

METHODS

The expression of ZAP-70 was analyzed in T-cell and B-cell lines and in peripheral-blood samples from 56 patients with CLL with the use of flow cytometry, Western blotting, and immunohistochemistry. The results were correlated with the IgV_H mutational status and clinical outcome.

RESULTS

ZAP-70 was detected by flow-cytometric analysis in cells of T-cell lineage and in leukemic cells from 32 of 56 patients with CLL. In all patients in whom at least 20 percent of the leukemic cells were positive for ZAP-70, IgV_H was unmutated, whereas IgV_H mutations were found in 21 of 24 patients in whom less than 20 percent of the leukemic cells were positive for ZAP-70 ($P<0.001$). Concordant results were obtained when ZAP-70 expression was assessed by immunohistochemistry or Western blotting. The level of ZAP-70 expression did not change over time (median, 37 months) in sequential samples from 30 patients with CLL. Patients with Binet stage A CLL who had at least 20 percent ZAP-70–positive leukemic cells had more rapid progression and poorer survival than those with less than 20 percent ZAP-70–positive cells.

CONCLUSIONS

Among patients with CLL, expression of ZAP-70, as detected by flow-cytometric analysis, correlated with IgV_H mutational status, disease progression, and survival.

From the Department of Hematology (M.C., F.B., A.L.-G., E.M.) and the Hematopathology Unit (N.V., B.B., D.C., M.R., S.M., E.C.), Institut d'Investigacions Biomèdiques August Pi i Sunyer, Hospital Clínic, Barcelona, Spain. Address reprint requests to Dr. Bosch at the Department of Hematology, Hospital Clínic, Villarroel 170, Barcelona 08036, Spain, or at fbosch@clinic.ub.es.

Ms. Crespo and Drs. Bosch and Villamor contributed equally to the article.

N Engl J Med 2003;348:1764-75.

THE STAGING SYSTEMS DEVELOPED BY Rai et al.[1] and Binet et al.[2] are standard methods of assessing prognosis in chronic lymphocytic leukemia (CLL). However, since these systems cannot identify stable or progressive forms of the disease, there has been a continual effort to identify other prognostic factors in CLL.[3-6]

About 50 to 70 percent of patients with CLL have evidence of somatic hypermutation in the immunoglobulin heavy-chain variable-region (IgV_H) genes of the leukemic cells.[7-11] These patients probably constitute a subgroup in whom the leukemic cells have passed through the germinal center, the site of IgV_H hypermutation.[12] It is important to note that patients with unmutated IgV_H genes usually have an advanced stage of CLL and unfavorable cytogenetic features, require therapy, and have a short survival. In contrast, patients with leukemic cells that have mutant IgV_H genes usually present in an early clinical stage, frequently have 13q14 chromosomal deletions, do not have alterations of p53, do not require therapy, and have a long survival.[11,13,14] For these reasons, knowledge of the mutational status of IgV_H is of considerable value in assessing the prognosis in CLL. Most general laboratories, however, are unable to determine IgV_H sequences. Moreover, even when the technique is available, it is too costly and time consuming to include in the standard workup of CLL. These considerations have made finding a surrogate for IgV_H mutational status in CLL an important priority.

Investigations using DNA microarrays[15,16] have shown that CLL cells exhibit a characteristic gene-expression profile in which the expression of a small subgroup of genes, including those encoding ZAP-70, IM1286077, and C-type lectin, correlates with the mutational status of IgV_H genes.[16,17] ZAP-70, a member of the Syk–ZAP-70 protein tyrosine kinase family, is normally expressed in T cells and natural killer cells and has a critical role in the initiation of T-cell signaling.[18-22] This finding led us to hypothesize that the expression of ZAP-70 could not only predict IgV_H mutational status but also serve as a prognostic factor in CLL. We therefore analyzed ZAP-70 protein in CLL cells from a series of patients using Western blotting, immunohistochemistry, and flow cytometry and correlated the results with the mutational status of the IgV_H genes and the clinical outcome.

METHODS

PATIENTS AND SAMPLE COLLECTION

Fifty-six patients who had received a diagnosis of CLL at our institution were selected on the basis of the availability of frozen samples for biologic studies. Lymph-node–biopsy specimens were available from eight patients. Progression was defined as a change to a more advanced clinical stage or the need for treatment. The time to progression and survival were calculated from the time of diagnosis. The median age was 60 years (range, 37 to 81), and the median duration of follow-up (from diagnosis) was 63 months.

Mononuclear cells from peripheral-blood samples were isolated on a Ficoll–Hypaque gradient (Seromed).[23] In three samples, CD19+ cells were isolated with use of anti-CD19 fluorescein isothiocyanate, followed by separation with anti–fluorescein isothiocyanate Microbeads (Miltenyi Biotec). Lymph-node–biopsy specimens from six additional patients who had received a diagnosis of mantle-cell lymphoma according to the criteria of the World Health Organization[24] were included in the analysis.

PREPARATION OF RNA, COMPLEMENTARY DNA, AND GENOMIC DNA

Total RNA was isolated with use of Ultraspec RNA (Biotecx Laboratories) according to the manufacturer's instructions. Complementary DNA (cDNA) was synthesized from 1 μg of RNA with the use of Moloney–murine leukemia virus reverse transcriptase (Invitrogen, Life Technologies). High-molecular-weight DNA was extracted from mononuclear cells isolated on a Ficoll gradient with use of a salting-out procedure.[25]

AMPLIFICATION OF IgV_H GENES

We amplified cDNA using a set of six heavy-chain variable-region (V_H) family-specific primers (V_H1 through V_H6) that anneal to sequences in the leader region[26] along with primers complementary to the constant region (IgM and IgG).[7] When amplification with these primers failed, an alternative set of primers specific to framework I region and the heavy-chain joining (J_H) region was used.[27] For the amplification of genomic DNA, approximately 100 ng of DNA was used in a total volume of 50 μl.[11]

IgV_H MUTATIONAL STATUS

Polymerase-chain-reaction (PCR) products were purified either directly with use of the Concert rap-

id PCR purification system (GIBCO BRL), or by gel excision with use of the QIAEX II agarose-gel extraction kit (Qiagen). Products were directly sequenced from both strands with use of the Big Dye Terminator Cycle Sequencing Ready Reaction (versions 2.0 and 3.0, Applied Biosystems) according to the manufacturer's instructions. Sequencing analysis and alignments were performed with use of DNAPLOT software and the VBASE data library.[28] Samples in which fewer than 2 percent of base pairs differed from those of the consensus sequence were considered unmutated.[8]

WESTERN BLOTTING

Western blotting of cell lysates was carried out as previously described.[23] Cell lysates from the following cell lines were also included: Jurkat (a T-cell line derived from lymphoblastic lymphoma), JVM-2 (B-cell prolymphocytic leukemia), Granta 519 and REC (mantle-cell lymphoma), DHL-16 and DOHH-2 (follicular lymphoma), Ly1.2 and Ly3 (diffuse large-B-cell lymphoma), and Namalwa, Raji, Daudi, and Ramos (Burkitt's lymphoma). Blots were incubated with anti–ZAP-70 antibody (Upstate Biotechnology) and anti–α-tubulin (Calbiochem). Lysates from Jurkat cells, a T-cell line with a high level of expression of ZAP-70 protein,[18] were used as a positive control. To analyze the influence of normal T cells present in the CLL samples, we mixed different concentrations of mononuclear cells from healthy blood donors with REC cells, a B-cell line that does not express ZAP-70.

IMMUNOHISTOCHEMISTRY

We also analyzed the expression of ZAP-70 in paraffin-embedded sections of lymph-node–biopsy specimens from eight patients with CLL and six patients with mantle-cell lymphoma using an anti–ZAP-70 antibody (ZAP-70-LR, Santa Cruz Biotechnology). We evaluated the level of ZAP-70 expression in tumor cells, T cells, and residual germinal-center areas.

FLOW CYTOMETRY

Mononuclear cells, as well as whole blood, from 56 patients with CLL and 10 healthy blood donors used as normal controls were fixed and permeabilized with use of the Fix & Perm kit (Caltag Laboratories) according to the manufacturer's instructions. Then 1.5 μg of anti–ZAP-70 antibody per 500,000 cells was incubated for 20 minutes at room temperature, washed twice in phosphate-buffered saline (Biomerieux), incubated for 20 minutes with goat antimouse immunoglobulin fluorescein isothiocyanate (Dako), washed, and then incubated with normal mouse serum for five minutes. Finally, CD3–phycoerythrin, CD56–phycoerythrin, CD19–peridinin chlorophyll protein cychrome 5.5, and CD5–allophycocyanine (BD Biosciences) were added, and the samples were incubated for 15 minutes. Samples were analyzed with a flow cytometer (FACS Calibur, BD Biosciences) with a gate on the fluorescence 2 detector to ensure that at least 1000 T cells and natural killer cells were analyzed in each sample. In samples from healthy control subjects, at least 5000 B cells were also analyzed. Analysis of stained samples was carried out with use of CellQuest software (BD Biosciences).

Lymphocytes were gated to avoid the inclusion of debris, monocytes, and doublets. The resultant cells were then gated to select CD3+CD56+ cells (T and natural killer cells), used as an internal control for ZAP-70 expression, and CD19+CD5+ (CLL cells). Biparametric dot graphs of cells that were stained for ZAP-70 and CD3 plus CD56 were independently plotted for T cells and natural killer cells and CLL cells. A marker that included T cells and natural killer cells (in the upper right quadrant of each graph) was used to calculate the percentage of CLL cells that were positive for ZAP-70. The percentage of CD19+ cells that also expressed CD38 was quantified as previously described.[8]

STATISTICAL ANALYSIS

Correlations between ZAP-70, CD38, and mutational status were analyzed with use of Wilcoxon's and Fisher's exact tests and a multiple regression analysis. To identify the level of ZAP-70 expression that could best be used to discriminate mutated from unmutated cells, we used a receiver-operating-characteristic plot.[29] Correlations between the clinical characteristics and the expression of ZAP-70 were also analyzed with use of Wilcoxon's or Fisher's exact test. Survival and time to progression were estimated according to the method of Kaplan and Meier and compared between groups by means of the log-rank test. All P values were two-sided, and the type I error was set at 5 percent. Statistical analyses were performed with use of SPSS software.[30]

RESULTS

SOMATIC MUTATIONS IN *IgV$_H$* GENES

All sequences of *IgV$_H$* genes in the leukemic cells from the 56 patients were in-frame rearrangements, and only two premature stop codons were observed. We

found somatic mutations (up to 98 percent homology with germ-line sequences) in 21 of 56 patients (38 percent), including 7 that had 95.6 to 97.3 percent homology with germ-line sequences (Table 1).

WESTERN BLOT ANALYSIS OF ZAP-70 EXPRESSION

ZAP-70 expression was analyzed in 12 human cell lines corresponding to different stages of B-cell differentiation. Peripheral-blood lymphocytes from healthy blood donors (data not shown) and the Jurkat T-cell line were used as positive controls. The protein was not detected in any of the B-cell lines, except the Ramos cell line, in which it was expressed weakly (Fig. 1A).

Of 32 samples from the patients with CLL, 16 had a high level of expression of ZAP-70 on Western blotting and the remaining 16 had a low level of expression (Fig. 1B). The presence of more than 2 percent T cells in the blood samples influenced the result, especially when the proportion was 10 percent or higher (Fig. 1C). However, samples from all but two patients with CLL contained less than 15 percent T cells on Western blotting (mean [±SD], 4.5±5.5 percent); Patient 45 had more than 20 percent T cells in the sample.

IMMUNOHISTOCHEMICAL ANALYSIS OF ZAP-70 EXPRESSION

We analyzed lymph-node–biopsy specimens from eight patients with CLL, none of whom had IgV_H mutations, and six patients with mantle-cell lymphoma, which is characterized by proliferation of CD5+ B cells but not usually by IgV_H mutations. All lymph-node–biopsy specimens from the patients with CLL were positive for ZAP-70, with a diffuse pattern reflecting the infiltration by leukemic cells. T cells in the biopsy specimens showed stronger immunoreactivity than the CLL cells. Residual germinal centers were negative for ZAP-70. All mantle-cell lymphomas were negative for ZAP-70, whereas T cells in the tissue had a high level of expression of ZAP-70.

FLOW-CYTOMETRIC ANALYSIS OF ZAP-70 EXPRESSION

In samples of normal blood, flow-cytometric analysis disclosed a population with high and homogeneous expression of ZAP-70 (Fig. 2A). This population corresponded to T cells and natural killer cells. In these samples, the proportion of normal B cells (from healthy blood donors) expressing as much ZAP-70 as T cells and natural killer cells was 0 to 6.5 percent (mean, 4±2.5). No significant differences in ZAP-70 expression were observed between CD5– and CD5+ B-cell subpopulations (Fig. 2B).

The method used to quantify the percentage of CLL cells expressing as much ZAP-70 as T cells is shown in Figure 2C. Leukemic cells from 56 patients with CLL were analyzed for ZAP-70 expression by flow cytometry. In these samples, T cells and natural killer cells also displayed high and homogeneous levels of expression of ZAP-70. In contrast to normal CD5+ B cells, CD5+ CLL cells from 32 of 56 patients expressed high levels of ZAP-70 (Fig. 2D).

In all but one patient (Patient 45), there was complete concordance of ZAP-70 expression as assessed by flow cytometry, Western blotting, and immunohistochemistry (Table 1). These discrepant results in Patient 45 (Fig. 1B and Table 1) could be explained by the high number of T cells (20 percent) in the patient's sample. ZAP-70 expression was also analyzed in 30 of 56 patients from whom two sequential samples were available. The median time between the collections of the samples was 37 months (range, 11 to 64). None of these 30 patients had significant changes in ZAP-70 expression over time.

CORRELATION BETWEEN ZAP-70 PROTEIN AND IgV_H MUTATIONAL STATUS

There was a strong correlation between the presence of IgV_H mutations and the percentage of leukemic cells that expressed ZAP-70, as assessed by flow cytometry. In the receiver-operating-characteristic analysis, a value of 17.5 percent ZAP-70–positive CLL cells was the best cutoff for assigning IgV_H mutational status. We used a cutoff value of 20 percent for simplicity. Patients with unmutated IgV_H genes had higher percentages of ZAP-70–positive CLL cells than did patients with IgV_H mutations (48± 21 percent vs. 6±4 percent, $P<0.001$). Samples from all 21 patients with IgV_H mutations contained less than 20 percent ZAP-70–positive CLL cells, and all but 3 patients without IgV_H mutations (91 percent) had 20 percent or more ZAP-70–positive CLL cells (Fig. 3A and 3B). Conversely, all the patients with increased proportions of ZAP-70–positive cells did not have somatic mutations, and 88 percent of patients with low numbers of ZAP-70–positive cells had IgV_H mutations. Overall, the probability of the absence of somatic mutations in the presence of more than 20 percent ZAP-70–positive CLL cells (positive predictive value) was 100 percent (95 percent confidence interval, 89 to 100), whereas the probability of IgV_H mutations in the presence of a low percentage of ZAP-70–positive cells (negative pre-

Table 1. Main Biologic and Clinical Characteristics of the Patients.*

Patient No.	IgV_H				ZAP-70 Expression			CD38+ Cells	Stage at Diagnosis		Survival
	Somatic Mutations	Homology	Family	No. of Nucleotide Changes	Western Blotting	Flow-Cytometric Analysis	IHC of Lymph-Node Biopsy Specimen		Binet	Rai	
		%				% *(category)*		%			*mo*
1	No	100	4–39	0	—	69 (high)	—	99	A	0	29
2	No	100	3–48	0	—	54 (high)	—	—	A	I	10
3	No	100	1–46	0	Strong	21 (high)	—	—	A	0	3†
4	No	100	1–69	0	—	47 (high)	—	4	A	I	61
5	No	100	3–23	0	—	60 (high)	Strong	95	B	II	74†
6	No	100	1–69	0	—	59 (high)	Strong	—	B	II	75†
7	No	100	3–33	0	—	61 (high)	—	99	A	I	60†
8	No	100	1–03	0	—	45 (high)	Strong	—	B	I	48†
9	No	100	1–69	0	—	29 (high)	—	—	A	0	48
10	No	100	1–03	0	—	64 (high)	—	46	A	0	58†
11	No	100	1–69	0	—	64 (high)	—	94	A	0	58
12	No	100	3–11	0	—	54 (high)	Strong	—	A	0	104
13	No	100	1–18	0	—	70 (high)	—	1	A	0	77
14	No	100	1–03	0	Strong	24 (high)	—	4	A	0	39†
15	No	100	1–e	0	Strong	37 (high)	—	64	C	IV	92
16	No	100	3–11	0	Strong	46 (high)	—	30	A	0	26†
17	No	100	1–69	0	Strong	46 (high)	—	11	A	0	84†
18	No	100	1–e	0	Strong	30 (high)	—	95	A	I	85†
19	No	100	2–70	0	Strong	74 (high)	—	—	A	0	76†
20	No	100	1–69	0	Strong	73 (high)	—	71	A	0	67†
21	No	100	3–30	0	Strong	60 (high)	—	70	A	I	80†
22	No	100	3–74	0	Strong	30 (high)	—	80	B	II	18
23	No	99.7	1–69	1	—	35 (high)	Strong	83	A	0	67†
24	No	99.6	4–34	1	Strong	77 (high)	—	50	A	I	49†
25	No	99.6	1–69	1	Strong	29 (high)	—	39	A	I	92†
26	No	99.3	1–69	2	Strong	73 (high)	Strong	53	A	I	67
27	No	99.3	3–49	2	—	73 (high)	Strong	99	A	0	78†
28	No	99.3	1–69	2	Strong	51 (high)	—	95	A	I	109†
29	No	99	3–09	3	Strong	70 (high)	—	53	A	0	307
30	No	98.6	3–48	4	—	71 (high)	—	99	A	0	19

Table 1. (Continued.)

Patient No.	IgV_H			ZAP-70 Expression				CD38+ Cells	Stage at Diagnosis		Survival
	Somatic Mutations	Homology	Family	No. of Nucleotide Changes	Western Blotting	Flow-Cytometric Analysis	IHC of Lymph-Node Biopsy Specimen		Binet	Rai	
		%				% *(category)*		%			*mo*
31	No	98.3	3–15	5	—	30 (high)	—	78	A	I	55†
32	No	98.3	1–69	5	—	29 (high)	Strong	86	B	II	80†
33‡	No	100	3–43	0	Weak	5 (low)	—	25	B	II	48†
34‡	No	100	1–69	0	Weak	5 (low)	—	50	C	IV	47
35‡	No	100	3–72	0	Weak	12 (low)	—	2	A	0	87†
36	Yes	97.3	4–61	8	Weak	12 (low)	—	15	B	II	8†
37	Yes	96.6	1–02	10	Weak	4 (low)	—	1	A	0	52†
38	Yes	96.2	4–59	11	Weak	1 (low)	—	0	A	0	138†
39	Yes	95.6	3–07	13	—	11 (low)	—	73	A	0	63†
40	Yes	95.6	4–31	13	—	7 (low)	—	—	A	0	46†
41	Yes	95.6	7–04.1	13	Weak	5 (low)	—	5	A	I	121†
42	Yes	95.6	4–61	13	Weak	2 (low)	—	1	C	IV	289†
43	Yes	93.9	3–21	9	Weak	13 (low)	—	46	A	III	25
44	Yes	93.7	2–05	18	Weak	3 (low)	—	98	A	0	67†
45‡	Yes	93.5	5–51	19	Strong	12 (low)	—	0	A	0	14†
46	Yes	93.3	3–72	20	—	2 (low)	—	78	A	0	64†
47	Yes	93.2	1–03	19	Weak	6 (low)	—	2	A	0	128†
48	Yes	92.5	3–23	22	—	10 (low)	—	—	A	I	59†
49	Yes	92.4	4–34	22	—	1 (low)	—	—	C	IV	9
50	Yes	92.4	4–04	22	—	6 (low)	—	8	A	0	127†
51	Yes	92.4	4–34	22	Weak	6 (low)	—	1	A	0	421†
52	Yes	90.6	4–34	27	Weak	6 (low)	—	12	A	0	122†
53	Yes	89.8	1–18	35	Weak	3 (low)	—	0	A	0	43†
54	Yes	89.1	3–23	32	—	1 (low)	—	—	C	III	56†
55	Yes	89.1	3–74	34	Weak	4 (low)	—	38	A	0	83†
56	Yes	88.4	3–30	34	Weak	4 (low)	—	0	A	0	31†

* Samples in which fewer than 2 percent of base pairs differed from those of the consensus sequence for immunoglobulin heavy-chain variable-region (IgV_H) genes were considered unmutated.[8] The level of ZAP-70 expression was considered to be high if at least 20 percent of chronic lymphocytic leukemia cells were positive for the protein. Survival was measured from the time of diagnosis. IHC denotes immunohistochemical analysis.

† The patient was still alive at the time of analysis.

‡ The results of IgV_H mutational analysis and ZAP-70 expression were discordant.

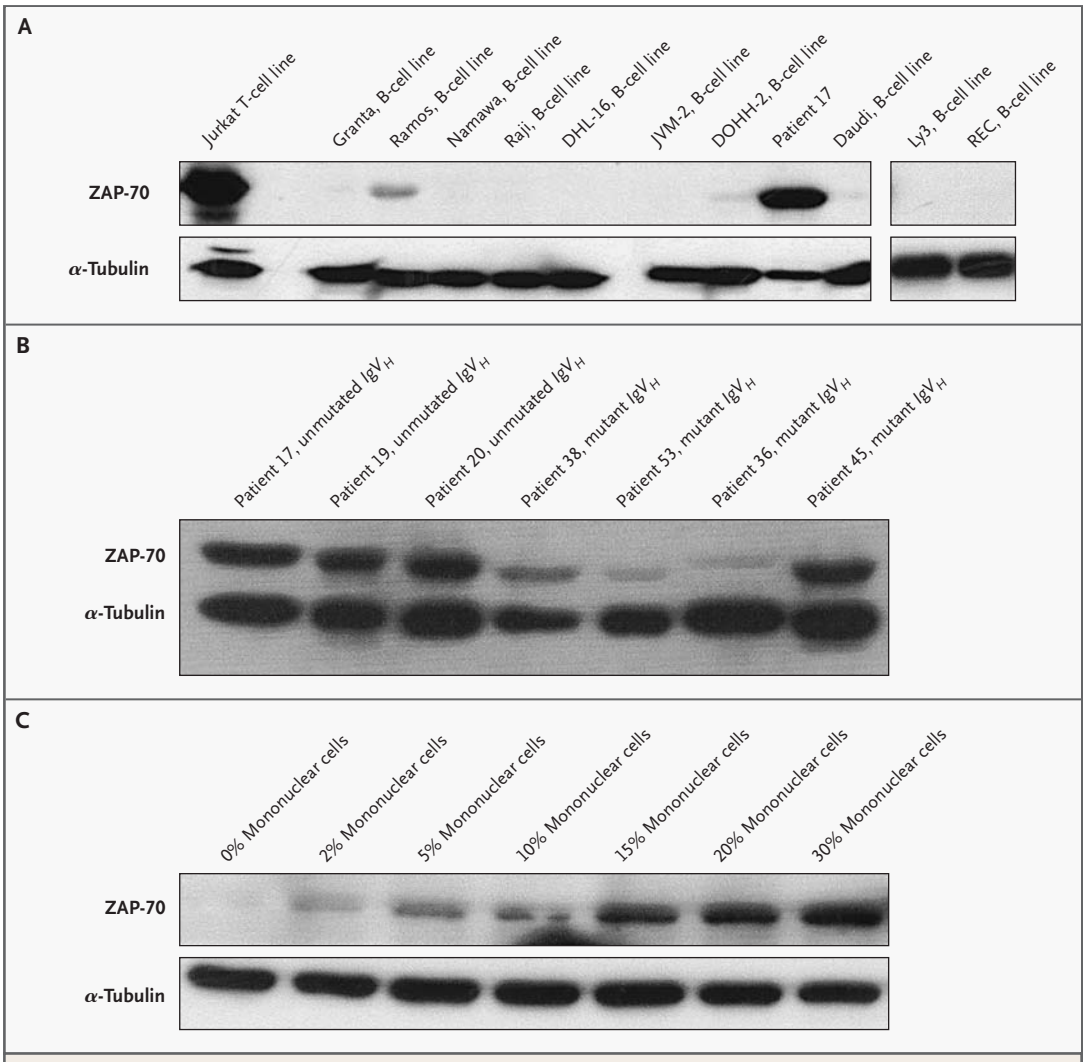

Figure 1. Western Blot Analysis of the Expression of ZAP-70 in a T-Cell Line, a Peripheral-Blood Sample from Patient 17 with Chronic Lymphocytic Leukemia (CLL), and 10 B-Cell Lines (Panel A); Seven Patients with CLL According to the Presence or Absence of Mutations in the Immunoglobulin Heavy-Chain Variable-Region (IgV_H) Genes (Panel B); and Normal Peripheral-Blood T Cells (Panel C).

In Panel A, only cells from the T-cell line Jurkat and Patient 17 showed a high level of expression of ZAP-70; the B-cell line Ramos exhibited weak expression. In Panel B, patients without IgV_H mutations — Patients 17, 19, and 20 — had a high level of ZAP-70 expression, whereas patients with IgV_H mutations had a low level of expression. Patient 45 had a high level of expression of ZAP-70 because of the high percentage of T cells (20 percent) in the sample. In Panel C, various concentrations (0 percent, 2 percent, 5 percent, 10 percent, 15 percent, 20 percent, and 30 percent) of mononuclear cells from healthy blood donors were mixed with REC cells, a B-cell line that does not express ZAP-70. The level of expression of ZAP-70 was barely visible in the sample containing 2 percent T cells and was high in the samples containing more than 10 percent T cells. In each panel, the expression of α-tubulin was used as a control.

dictive value) was 87.5 percent (95 percent confidence interval, 68 to 97). The sensitivity and specificity of the flow-cytometric analysis were 91 percent (95 percent confidence interval, 77 to 98) and 100 percent (95 percent confidence interval, 84 to 100), respectively.

To verify ZAP-70 expression in the three patients in whom IgV_H status and flow-cytometric results were discordant, Western blot analysis was performed on isolated fractions of CD19+ cells with a purity greater than 98 percent (CD19 is a surface marker of B cells). A weak signal was observed in all

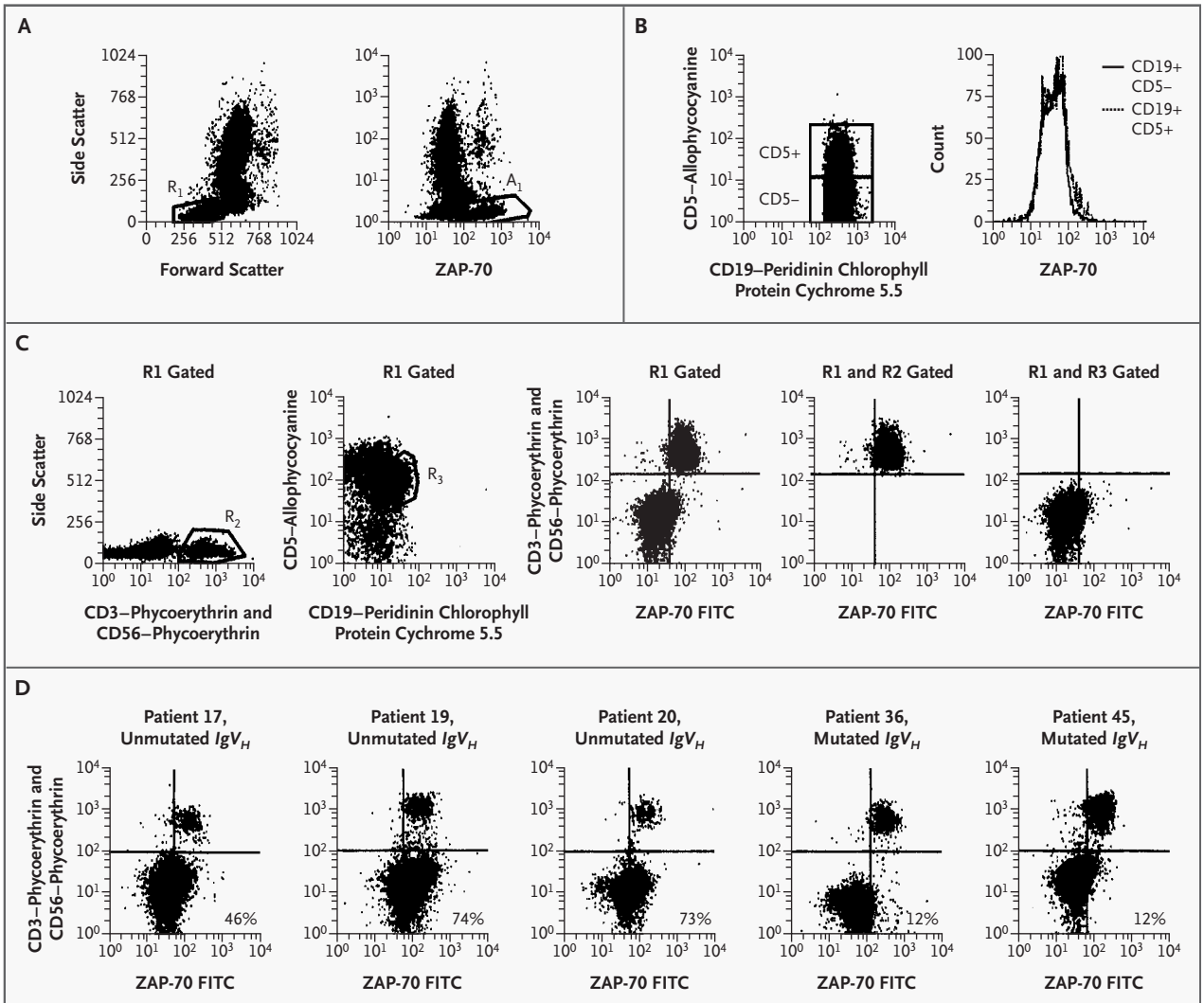

Figure 2. Immunofluorescence and Flow-Cytometric Analysis of the Expression of ZAP-70.

Panel A shows flow-cytometric plots of lysed whole blood. In the left-hand plot, forward and side scatter of lysed blood is represented with a region (R1) drawn around the lymphocytes. The right-hand plot shows side scatter and ZAP-70 staining of the same sample; A_1 denotes a population with a low SSC and a high level of expression of ZAP-70. Panel B shows the level of expression of ZAP-70 by normal B cells. The left-hand plot shows the expression of CD5 on gated CD19+ cells, with two regions showing the CD5+ and CD5– B-cell subpopulations. The histogram on the right-hand side represents the expression of ZAP-70 by the CD19+CD5– subpopulation and the CD19+CD5+ subpopulation. Panel C shows the method used to quantify the expression of ZAP-70 by chronic lymphocytic leukemia (CLL) cells. Lymphocytes were R1 gated, and then T cells and natural killer (CD3+CD56+) cells (the R2 region in the leftmost plot) and CLL (CD19+CD5+) cells (the R3 region in the second plot) were selected according to their phenotype. The third plot shows the expression of ZAP-70 after lymphocyte (R1) gating. For the purposes of quantification, markers were placed so that the T cells and natural killer cells (R1 and R2 gated) with a high level of expression of ZAP-70 would appear in the upper right quadrant (fourth plot). Subsequently, CLL cells were plotted, and the cells in the lower right quadrant were quantified as CLL cells with a high level of expression of ZAP-70 (rightmost plot). Panel D shows the level of expression of ZAP-70 by lymphocytes from five representative patients with CLL according to the mutational status of immunoglobulin heavy-chain variable-region (IgV_H) genes. The percentage of CLL cells with a high level of expression of ZAP-70 is shown in the lower right quadrant of each plot, after the exclusion of T cells and natural killer cells. FITC denotes fluorescein isothiocyanate.

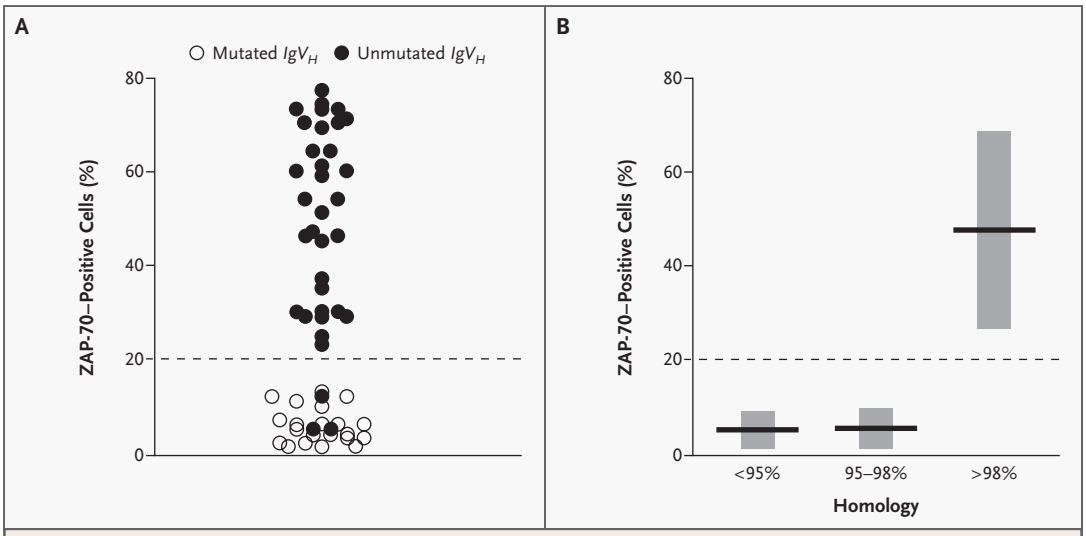

Figure 3. Correlation of the Level of Expression of ZAP-70 and Immunoglobulin Heavy-Chain Variable-Region (IgV_H) Mutational Status (Panel A) and IgV_H Sequence Homology (Panel B).

Panel A shows a scatter plot representing the levels of ZAP-70 expression measured by flow-cytometric analysis and the IgV_H mutational status of the 56 patients analyzed. When the threshold for categorizing ZAP-70 was established at 20 percent, two subgroups were clearly delineated: patients with unmutated IgV_H and a high level of ZAP-70 expression and patients with mutant IgV_H and low levels of ZAP-70 expression. Only three patients without IgV_H mutations had low levels of ZAP-70 expression. Panel B shows the mean (±SD) (horizontal line and box) level of expression of ZAP-70 according to the degree of homology of each IgV_H sequence with the consensus sequence (less than 95 percent, 95 to 98 percent, or more than 98 percent). There were no significant differences in the level of ZAP-70 expression between the subgroup with less than 95 percent sequence homology and the subgroup with 95 to 98 percent sequence homology.

three samples (data not shown), validating the low levels of expression of ZAP-70 observed on flow cytometry.

ZAP-70 AND CD38 EXPRESSION

Data for the expression of CD38 were available for 45 patients (CD38 is a marker that has been proposed as a surrogate for IgV_H mutational status). Of these 45 patients, 18 had no more than 30 percent CD38+ cells (Table 1). There were significant differences in the mean percentages of CD38+ CLL cells between patients with IgV_H mutations and those without IgV_H mutations (20 percent vs. 60 percent, P<0.001). In addition, 22 of 28 patients without IgV_H mutations (79 percent) had at least 30 percent CD38+ cells, whereas 12 of 17 (71 percent) with somatic mutations had less than 30 percent CD38+ cells. Moreover, the percentage of CD38+ cells was at least 30 percent in 21 of 25 patients (84 percent) with at least 20 percent ZAP-70–positive cells and less than 30 percent in 14 of 20 patients (70 percent) with less than 20 percent ZAP-70–positive cells. The level of CD38 expression was also low in the two patients with discordant results of ZAP-70 expression and IgV_H mutations (Table 1). In a multiple regression analysis, only ZAP-70 expression (P<0.001), and not CD38 expression, maintained its correlation with IgV_H mutational status.

PROGNOSTIC IMPORTANCE OF THE PERCENTAGE OF ZAP-70–POSITIVE CELLS

None of the standard variables were associated with ZAP-70 expression, including Binet's and Rai's clinical stages, the lymphocyte count, and the lymphocyte doubling time. However, an increased percentage of ZAP-70–positive cells was associated with a short time to progression. Among 44 patients with Binet stage A, the median time to progression was 29 months for the 26 patients with at least 20 percent ZAP-70–positive cells, whereas the median was not reached among the 18 patients with less than 20 percent ZAP-70–positive cells (P=0.009) (Fig. 4A).

When survival was calculated from the time of diagnosis, the 26 patients with Binet stage A CLL and at least 20 percent ZAP-70–positive cells had a median survival of 90 months, whereas the median sur-

vival was not reached in the 18 patients with Binet stage A and less than 20 percent ZAP-70–positive cells (P=0.01) (Fig. 4B). However, when all patients were analyzed (Binet stage A, B, and C), the percentage of ZAP-70–positive cells was not significantly correlated with survival (P=0.06). The percentage of CD38+ cells (with a cutoff of 30 percent) did not predict progression or survival (data not shown). Finally, as expected, IgV_H mutational status also correlated with progression and survival (data not shown).

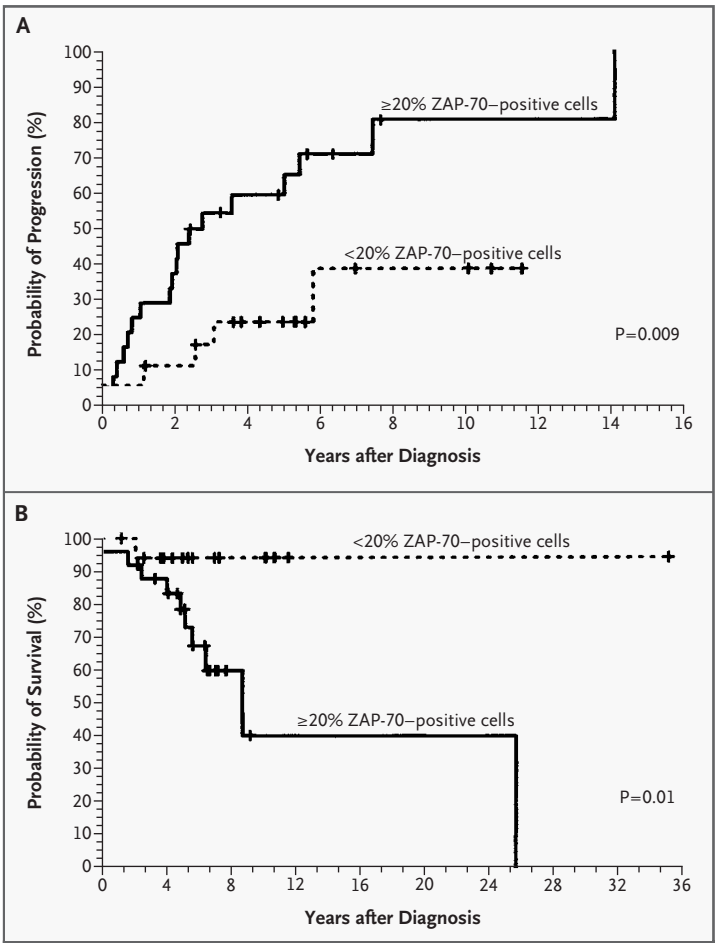

Figure 4. Kaplan–Meier Estimates of the Actuarial Risk of Disease Progression (Panel A) and the Likelihood of Survival (Panel B) among Patients with Binet Stage A Chronic Lymphocytic Leukemia, According to the Level of Expression of ZAP-70.

In Panel A, the median time to progression among 26 patients with a high level of ZAP-70 expression (20 percent or more) was 29 months, whereas it was not reached in 18 patients with a low level of ZAP-70 expression (less than 20 percent) (P=0.009). In Panel B, the probability of survival at 10 years was 90 percent among patients with a low level of ZAP-70 expression. The median survival was 90 months among the patients with a high level of ZAP-70 expression, whereas it was not reached among patients with a low level of ZAP-70 expression (P=0.01). Tick marks indicate censored data.

DISCUSSION

The management of CLL is based on each patient's individual risk, because the disease has a widely variable clinical course. An important determinant of the prognosis is the mutational status of IgV_H genes in the leukemic cells, which correlates with the clinical outcome better than and independently of classic prognostic factors.[8,11,31] Methods to identify IgV_H mutations are, however, not widely available in clinical practice. Our study confirms that the leukemic cells without IgV_H mutations in patients with CLL express high levels of ZAP-70, whereas the leukemic cells with IgV_H mutations in patients with CLL have barely detectable levels of ZAP-70.[16,17] Moreover, using flow cytometry, we found that none of the patients with CLL and at least 20 percent ZAP-70–positive cells had IgV_H somatic mutations, whereas all but three patients with less than 20 percent ZAP-70–positive cells had mutated IgV_H genes. Flow-cytometric analysis of ZAP-70 expression was a sensitive and specific surrogate for mutational status of IgV_H genes; this method should be readily available in general laboratories.

The mechanisms accounting for the relation between ZAP-70 expression and the mutational status of IgV_H are unknown. We also have no explanation for the inconsistency between mutational status and ZAP-70 levels in three of our patients. A discrepancy between ZAP-70 expression, as assessed by Western blotting, and the IgV_H mutational status was also found in 1 of 22 patients in another series.[17]

Apart from CLL cells, ZAP-70 was expressed only in T cells and tumors of T-cell lineage, whereas it was barely detectable in normal CD19+CD5+ cells. It was not detected by Western blotting or immunohistochemistry in any of the B-cell lines or biopsy specimens of mantle-cell lymphoma. Nevertheless, ZAP-70 messenger RNA has been found in other B-cell lines with the use of reverse-transcriptase–PCR (RT-PCR) analysis.[16] Our results indicate that, among B-cell and T-cell lymphoproliferative disorders, a high level of ZAP-70 expression is restricted to T-cell proliferative diseases and a subgroup of CLL.

The use of flow cytometry to assess the level of ZAP-70 expression offers advantages over other systems of analysis. With flow cytometry, it is possible

to analyze the percentage of ZAP-70–positive cells selectively in subpopulations of CLL cells, T cells, and natural killer cells. By contrast, Western blotting and RT-PCR can overestimate the level of expression of ZAP-70 owing to the presence of T cells in the sample.[16,17]

The value of CD38 as a surrogate for IgV_H mutations is controversial.[32,33] Moreover, the level of CD38 expression may vary over the course of the disease.[34] In our series, the level of CD38 expression did not correlate with disease progression or survival. In contrast, the level of expression of ZAP-70 did not change over time, and the presence of ZAP-70 was associated with rapid progression and poor survival.

In conclusion, the expression of ZAP-70 by CLL cells, as ascertained by flow-cytometric analysis, is a simple and reliable surrogate for the identification of IgV_H mutations. Moreover, ZAP-70 expression by itself can be used as a prognostic marker. For these reasons, ZAP-70 analysis should be included in the workup of patients with CLL.

Supported in part by grants from the José Carreras International Foundation against Leukemia (EM/02 and CR/02), Fondo de Investigaciones Sanitarias (02/0250 and 01/1581), and Ministerio de Ciencia y Tecnologia (SAF-02-3261). Ms. Crespo is a recipient of a grant from Fondo de Investigaciones Sanitarias, Spain.

We are indebted to Professor Freda K. Stevenson for technical advice in the analysis of the somatic mutations of IgV_H, to Montse Sánchez for immunohistochemical analysis, and to Penelope Elvy and Eoin McGrath for their assistance in the preparation of the manuscript.

REFERENCES

1. Rai KR, Sawitsky A, Cronkite EP, Chanana AD, Levy RN, Pasternack BS. Clinical staging of chronic lymphocytic leukemia. Blood 1975;46:219-34.
2. Binet JL, Auquier A, Dighiero G, et al. A new prognostic classification of chronic lymphocytic leukemia derived from a multivariate survival analysis. Cancer 1981;48:198-206.
3. Rozman C, Montserrat E. Chronic lymphocytic leukemia. N Engl J Med 1995;333:1052-7. [Erratum, N Engl J Med 1995;333:1515.]
4. Caligaris-Cappio F, Hamblin TJ. B-cell chronic lymphocytic leukemia: a bird of a different feather. J Clin Oncol 1999;17:399-408.
5. Montserrat E. Classical and new prognostic factors in chronic lymphocytic leukemia: where to now? Hematol J 2002;3:7-9.
6. Döhner H, Stilgenbauer S, Benner A, et al. Genomic aberrations and survival in chronic lymphocytic leukemia. N Engl J Med 2000;343:1910-6.
7. Fais F, Ghiotto F, Hashimoto S, et al. Chronic lymphocytic leukemia B cells express restricted sets of mutated and unmutated antigen receptors. J Clin Invest 1998;102:1515-25.
8. Damle RN, Wasil T, Fais F, et al. Ig V gene mutation status and CD38 expression as novel prognostic indicators in chronic lymphocytic leukemia. Blood 1999;94:1840-7.
9. Schroeder HW Jr, Dighiero G. The pathogenesis of chronic lymphocytic leukemia: analysis of the antibody repertoire. Immunol Today 1994;15:288-94.
10. Oscier DG, Thompsett A, Zhu D, Stevenson FK. Differential rates of somatic hypermutation in V(H) genes among subsets of chronic lymphocytic leukemia defined by chromosomal abnormalities. Blood 1997;89:4153-60.
11. Hamblin TJ, Davis Z, Gardiner A, Oscier DG, Stevenson FK. Unmutated Ig V(H) genes are associated with a more aggressive form of chronic lymphocytic leukemia. Blood 1999;94:1848-54.
12. Rajewsky K. Clonal selection and learning in the antibody system. Nature 1996;381:751-8.
13. Stilgenbauer S, Bullinger L, Lichter P, Dohner H. Genetics of chronic lymphocytic leukemia: genomic aberrations and V(H) gene mutation status in pathogenesis and clinical course. Leukemia 2002;16:993-1007.
14. Lin K, Sherrington PD, Dennis M, Matrai Z, Cawley JC, Pettitt AR. Relationship between p53 dysfunction, CD38 expression, and IgV(H) mutation in chronic lymphocytic leukemia. Blood 2002;100:1404-9. [Erratum, Blood 2002;100:2291.]
15. Klein U, Tu Y, Stolovitzky GA, et al. Gene expression profiling of B cell chronic lymphocytic leukemia reveals a homogeneous phenotype related to memory B cells. J Exp Med 2001;194:1625-38.
16. Rosenwald A, Alizadeh AA, Widhopf G, et al. Relation of gene expression phenotype to immunoglobulin mutation genotype in B cell chronic lymphocytic leukemia. J Exp Med 2001;194:1639-47.
17. Chen L, Widhopf G, Huynh L, et al. Expression of ZAP-70 is associated with increased B-cell receptor signaling in chronic lymphocytic leukemia. Blood 2002;100:4609-14.
18. Chan AC, Irving BA, Fraser JD, Weiss A. The zeta chain is associated with a tyrosine kinase and upon T-cell antigen receptor stimulation associates with ZAP-70, a 70-kDa tyrosine phosphoprotein. Proc Natl Acad Sci U S A 1991;88:9166-70.
19. Chan AC, Iwashima M, Turck CW, Weiss A. ZAP-70: a 70 kd protein-tyrosine kinase that associates with the TCR zeta chain. Cell 1992;71:649-62.
20. Vivier E, da Silva AJ, Ackerly M, et al. Association of a 70-kDa tyrosine phosphoprotein with the CD16: zeta:gamma complex expressed in human natural killer cells. Eur J Immunol 1993;23:1872-6.
21. Isakov N, Wange RL, Burgess WH, Watts JD, Aebersold R, Samelson LE. ZAP-70 binding specificity to T cell receptor tyrosine-based activation motifs: the tandem SH2 domains of ZAP-70 bind distinct tyrosine-based activation motifs with varying affinity. J Exp Med 1995;181:375-80.
22. Latour S, Veillette A. Proximal protein tyrosine kinases in immunoreceptor signaling. Curr Opin Immunol 2001;13:299-306.
23. Bellosillo B, Villamor N, Lopez-Guillermo A, et al. Spontaneous and drug-induced apoptosis is mediated by conformational changes of Bax and Bak in B-cell chronic lymphocytic leukemia. Blood 2002;100:1810-6.
24. Swerdlow SH, Berger F, Isaacson PI, et al. Mature B-cell neoplasms: mantle cell lymphoma. In: Jaffe ES, Harris NL, Stein H, Vardiman JW, eds. Pathology and genetics of tumours of haematopoietic and lymphoid tissues. WHO Classification of Tumours. Lyons, France: IARC Press, 2001:168-70.
25. Miller SA, Dykes DD, Polesky HF. A simple salting out procedure for extracting DNA from human nucleated cells. Nucleic Acids Res 1988;16:1215.
26. Campbell MJ, Zelenetz AD, Levy S, Levy R. Use of family specific leader region primers for PCR amplification of the human heavy chain variable region gene repertoire. Mol Immunol 1992;29:193-203.
27. Deane M, Norton JD. Immunoglobulin heavy chain variable region family usage is independent of tumor cell phenotype in human B lineage leukemias. Eur J Immunol 1990;20:2209-17.
28. Cook GP, Tomlinson IM. The human immunoglobulin VH repertoire. Immunol Today 1995;16:237-42.
29. Zweig MH, Campbell G. Receiver-operating characteristics (ROC) plots: a fundamental evaluation tool in clinical medicine. Clin Chem 1993;39:561-77. [Erratum, Clin Chem 1993;39:1589.]
30. SPSS advanced statistics, version

10.0.6. Chicago, SPSS, 1999 (software).
31. Oscier DG, Gardiner AC, Mould SJ, et al. Multivariate analysis of prognostic factors in CLL: clinical stage, IgV_H gene mutational status, and loss or mutation of the p53 gene are independent prognostic factors. Blood 2002;100:1177-84.
32. Del Poeta G, Maurillo L, Venditti A, et al. Clinical significance of CD38 expression in chronic lymphocytic leukemia. Blood 2001; 98:2633-9.
33. Ibrahim S, Keating M, Do KA, et al. CD38 expression as an important prognostic factor in B-cell chronic lymphocytic leukemia. Blood 2001;98:181-6.
34. Hamblin TJ, Orchard JA, Gardiner A, Oscier DG, Davis Z, Stevenson FK. Immunoglobulin V genes and CD38 expression in CLL. Blood 2000;95:2455-7.

Spontaneous and drug-induced apoptosis is mediated by conformational changes of Bax and Bak in B-cell chronic lymphocytic leukemia

Beatriz Bellosillo, Neus Villamor, Armando López-Guillermo, Silvia Marcé, Francesc Bosch, Elias Campo, Emili Montserrat, and Dolors Colomer

The role of Bax and Bak, 2 proapoptotic proteins of the Bcl-2 family, was analyzed in primary B-cell chronic lymphocytic leukemia (CLL) cells following in vitro treatment with fludarabine, dexamethasone, or the combination of fludarabine with cyclophosphamide and mitoxantrone (FCM). A strong correlation was found between the number of apoptotic cells and the percentage of cells stained with antibodies recognizing conformational changes of Bax (n = 33; $r = 0.836$; $P < .001$) or Bak (n = 10; $r = 0.948$; $P < .001$). Preincubation of CLL cells with Z-VAD.fmk (N-benzyloxycarbonyl-Val-Ala-Asp-fluoromethyl ketone), a broad caspase inhibitor, abolished caspase-3 activation, exposure of phosphatidylserine residues, and reactive oxygen species generation; partially reversed the loss of transmembrane mitochondrial potential ($\Delta\Psi m$); but did not affect Bax or Bak conformational changes. These results indicate that the conformational changes of Bax and Bak occur upstream of caspase activation or are caspase independent. Following drug-induced apoptosis, Bax integrates into mitochondria, as demonstrated by fluorescence microscopy and Western blot, without changes in the total amount of Bax or Bak protein. Fludarabine and FCM induce p53 stabilization, but do not seem to be essential in inducing Bax and Bak conformational changes, as they are also observed in dexamethasone-treated CLL cells. These results demonstrate that, in CLL cells, the change in the intracellular localization of Bax from cytosol to mitochondria and the conformational changes of Bax and Bak are among the early steps in the induction of cell death. (Blood. 2002;100:1810-1816)

Introduction

B-cell chronic lymphocytic leukemia (CLL), the most common adult leukemia in Western countries, is characterized by the accumulation of long-lived, functionally inactive, mature-appearing neoplastic B-lymphocytes.[1] The clonal excess of B-cells is caused mainly by a decrease in cell death rather than by increased cell proliferation.[2] Although no curative treatment is currently available for CLL patients, several drugs have shown high activity against the disease, including purine analogs, glucocorticoids, alkylating agents, or combinations of these drugs.[3] Experimental evidence indicates that in CLL cells these drugs exert their cytotoxic effects mainly by inducing apoptosis.[4-7]

Signal transduction pathways involved in drug-induced apoptosis converge on a common pathway that consists of effector molecules (caspases), adaptor molecules (Apaf-1), and regulatory molecules (Bcl-2 family members, inhibitors of apoptosis [IAPs], and second mitochondria–derived activator of caspase/DIABLO [smac/DIABLO]). The integration of this cell death machinery takes place in the mitochondrion. Thus, in response to an apoptotic signal, the outer mitochondrial membrane is permeabilized, and this results in the release of cytochrome c, among other effects. Cytochrome c binds to Apaf-1 and results in the recruitment and activation of caspase-9, which subsequently activates downstream effectors, such as caspase-3.[8] Bcl-2 family proteins are major regulators of mitochondria-dependent apoptosis. The members of this family contain up to 4 highly conserved sequence regions and can be divided into 3 subgroups: antiapoptotic members, such as Bcl-2 and Mcl-1, with Bcl-2 sequence homology (BH) at BH1, BH2, BH3, and BH4 domains; proapoptotic proteins, such as Bax and Bak, with sequence homology at BH1, BH2, and BH3 domains; and, finally, proapoptotic proteins that share only the BH3 domain, such as Bid, Bik, Noxa, and Bim.[9]

Certain proapoptotic and antiapoptotic members, such as Bcl-2, Bcl-X_L, and Bak, reside predominantly in the mitochondria, whereas other members such as Bax, Bid, and Bad reside in the cytosol of healthy cells.[9] Recently, it has been proposed that translocation of Bax into the outer mitochondrial membrane plays a key role in the induction of cell death machinery.[10] Bax translocation involves a conformational change that exposes the NH_2-terminus and the hydrophobic COOH-terminus that targets mitochondria.[11,12] Bak is another proapoptotic member that is implicated in cell death induction. Similarly to Bax, up-regulation or conformational changes of Bak seem to be necessary to induce apoptosis.[13]

CLL cells contain high levels of the antiapoptotic Bcl-2 protein.[14] Increased ratios of Bcl-2 relative to its proapoptotic antagonist Bax have been correlated with refractory disease, progression of the disease, and shorter survival.[15-17] Higher levels

From the Departments of Hematology and Pathology, Institute of Hematology and Oncology from Hospital Clínic, Postgraduate School of Hematology Farreras-Valentí; Institut d'Investigacions Biomèdiques August Pi i Sunyer; and University of Barcelona, Spain.

Submitted December 27, 2001; accepted April 23, 2002. Prepublished online as *Blood* First Edition Paper, May 13, 2002; DOI 10.1182/blood-2001-12-0327.

Supported in part by FIS grants 99/0189 and 00/0946; José Carreras International Foundation Against Leukemia (EM/P-01); Roche España; and the Asociación Española Contra el Cáncer. B.B. and S.M. are recipients of a research fellowship from the Instituto de Salud Carlos III and Fondo de Investigaciones Sanitarias, respectively. Roche España provides funds for the research activities of the Institute of Hematology and Oncology.

Reprints: Emili Montserrat, Department of Hematology, Hospital Clínic, Villarroel 170, 08036 Barcelona, Spain; e-mail: emontse@clinic.ub.es.

The publication costs of this article were defrayed in part by page charge payment. Therefore, and solely to indicate this fact, this article is hereby marked "advertisement" in accordance with 18 U.S.C. section 1734.

of the antiapoptotic protein Mcl-1 have also been correlated with the failure to achieve complete remission in patients treated with alkylating agents or purine analogs.[18] Moreover, a decrease in Bcl-2 and Mcl-1 proteins and an increase in Bax and p53 proteins were observed following in vitro incubation of CLL cells with fludarabine.[7,19]

The aim of this study was to analyze the role of Bax and Bak in response to drug-induced cytotoxicity in CLL. For this purpose, conformational changes of Bax and Bak, its cellular redistribution, and modifications of other apoptosis-related proteins were analyzed in primary CLL cells following in vitro incubation with several drugs.

Patients, materials, and methods

Patients

The study included 33 patients (15 men and 18 women) with a median age of 65 years diagnosed with CLL. The diagnosis was established according to the World Health Organization classification.[20] All patients were informed of the investigational nature of this study, and informed consent was obtained from each patient in accordance with Hospital Clinic Ethical Committee (Barcelona, Spain).

Reagents

Fludarabine monophosphate was obtained from Schering (Berlin, Germany); mafosfamide from ASTAMedica (Frankfurt, Germany); mitoxantrone from Lederle Laboratories (Gosport, Hampshire, United Kingdom); dexamethasone from Merck (Darmstadt, Germany); and Z-VAD.fmk (N-benzyloxycarbonyl-Val-Ala-Asp-fluoromethyl ketone) from Bachem (Bubendorf, Switzerland).

Antibodies

The following antibodies were used: mouse monoclonal anti–cytochrome c (clones 7H8.2C12 and 6H2.B4) (BD-Pharmingen, San Diego, CA); rabbit polyclonal anti–caspase-3, active form (BD-Pharmingen); rabbit polyclonal anti-Bax antibody directed against amino acids 43 through 61 (BD-Pharmingen); rabbit polyclonal anti-Bax antibodies (N20 and Δ21) (Santa Cruz Biotechnology, CA); rabbit polyclonal anti-Bax against amino acids 1 through 20 (Upstate Biotechnology, Lake Placid, NY); mouse monoclonal anti-Bax antibody (clone YTH-6A7) (Trevigen, Gaithersburg, MD); mouse monoclonal anti-Bak antibodies (clone G317-1) (BD-Pharmingen) (Ab-1) (Oncogene Research Products, Boston, MA); polyclonal rabbit antibody generated against residues 2-14 of human Bak (Calbiochem-Novabiochem, San Diego, CA); rabbit polyclonal anti–Mcl-1 antibody (S-19) (Santa Cruz Biotechnology); mouse monoclonal anti–Bcl-2 antibody (DAKO, Glostrup, Denmark); mouse monoclonal anti-p53 antibodies (clone DO7) (DAKO) (Ab-2) (Oncogene Research Products); and rabbit polyclonal anti–poly–adenosine diphosphate ribose polymerase (PARP) antibody (Roche Diagnostics, Mannheim, Germany).

Isolation and culture of cells

Mononuclear cells were isolated from peripheral blood samples by centrifugation on a Ficoll/Hypaque (Seromed, Berlin, Germany) gradient and either used directly or cryopreserved in liquid nitrogen in the presence of 10% dimethyl sulfoxide. Manipulation due to freezing/thawing did not influence the cell response. Lymphocytes were cultured at a cell concentration of 5×10^6/mL in RPMI 1640 culture medium supplemented with 10% heat-inactivated fetal calf serum (Gibco BRL, Paisley, Scotland), 2 mM glutamine, and 60 μM (0.04 mg/mL) gentamicin, at 37°C in a humidified atmosphere containing 5% carbon dioxide. Cells were incubated for 24 hours with 5 μg/mL fludarabine; 10 μM dexamethasone; or the combination of 1 μg/mL fludarabine with 1 μg/mL mafosfamide, the active form of cyclophosphamide in vitro, and 0.5 μg/mL mitoxantrone (FCM).

Analysis of cell viability by annexin V binding

Exposure of phosphatidylserine residues was quantified by surface annexin V staining as previously described.[7] Briefly, cells were washed in binding buffer (10 mM HEPES [N-2-hydroxyethylpiperazine-N′-2-ethanesulfonic acid], pH 7.4; 2.5 mM $CaCl_2$; and 140 mM NaCl); resuspended in 200 μL; and incubated with 0.5 μg/mL annexin V–fluorescein isothiocyanate (FITC) (Bender Medsystems, Vienna, Austria) for 15 minutes in the dark. Cells were washed again and resuspended in binding buffer. Then 5 μL (20 μg/mL) propidium iodide (Sigma Chemicals, St Louis, MO) was added to each sample prior to flow cytometric analysis (FACScan; Becton Dickinson, Palo Alto, CA). Ten thousand cells per sample were acquired with the use of CELLquest software (Becton Dickinson), and data were analyzed with the Paint-a-gate Pro software (Becton Dickinson). All experiments were performed in duplicate.

Assessment of mitochondrial transmembrane potential ($\Delta\Psi_m$) and reactive oxygen species (ROS)

As previously described,[21] changes in $\Delta\Psi_m$ were evaluated by staining with 1 nM 3,3′-dihexyloxacarbocyanine iodide ($DiOC_6$[3]) (Molecular Probes, Eugene, OR). ROS production was determined by staining with 2 μM dihydroethidine (DHE) (Molecular Probes). Cells were incubated with the dyes for 15 minutes at 37°C, washed, resuspended in phosphate-buffered saline (PBS), and analyzed by flow cytometry. There were 10 000 cells acquired in a FACScan flow cytometer. All experiments were performed in duplicate.

Flow cytometric detection of intracellular proteins

Cells were fixed and permeabilized by means of the Cytofix/Cytoperm kit (BD-Pharmingen) for 20 minutes at 4°C, pelleted, and washed with Perm/Wash buffer (BD-Pharmingen). Cells were then stained with the antibodies against the active form of caspase-3, Bax, Bak, cytochrome c, or Bcl-2 (0.25 μg/L $\times 10^6$ cells) for 20 minutes at room temperature; washed in Perm/Wash buffer; stained with goat antirabbit-FITC (SuperTechs, Bethesda, MD), goat antimouse-FITC (DAKO), or goat antimouse-phycoerythrin (PE; DAKO); and analyzed in a FACScan. For p53 (clone DO7) detection, cellular fixation was performed in 0.5% paraformaldehyde and 80% ethanol at 4°C for at least 1 hour.

Western blot

Cells were lysed in 80 mM Tris (tris-(hydroxymethyl)-aminomethane) HCl, pH 6.8; 2% sodium dodecyl sulfate (SDS); 10% glycerol; and 0.1 M DTT (dithiothreitol); equal amounts of protein were separated by electrophoresis on 12% polyacrylamide gel and transferred to Immobilon-P (Millipore, Bedford, MA) membranes. The membranes were incubated with the indicated antibodies, and antibody binding was detected with the use of secondary antibodies conjugated to horseradish peroxidase and an enhanced chemiluminiscence (ECL) detection kit (Amersham, Buckinghamshire, United Kingdom). Mitochondrial and cytosolic protein extracts were obtained from 50×10^6 cells per condition by means of the ApoAlert cell fractionation kit (CLONTECH Laboratories, Palo Alto, CA). In some cases, pelleted mitochondria were incubated in 0.1 M Na_2CO_3, pH 11.5, for 20 minutes on ice and centrifuged to separate supernatants and mitoplasts.[22]

Statistical analysis

Correlations between Bax-positive and Bak-positive staining and other parameters of cell death, as well as correlation between Bax and Bak conformational changes, were analyzed by means of the Pearson correlation test or, when appropriate, the nonparametric Spearman test, with the use of the SPSS 10.0 software package (Chicago, IL). Differences between apoptosis induced by drugs were analyzed by the Wilcoxon nonparametric test.

Results

Drug-induced apoptosis is associated with conformational changes of Bax

Lymphocytes from 33 CLL patients were incubated with fludarabine, dexamethasone, or the FCM combination. As previously demonstrated,[7,23] these drugs decreased cell viability and induced the characteristic features of apoptosis. The number of apoptotic cells, assessed by annexin V binding, was higher in FCM-treated cells (61% ± 22.5%) than in cells treated with fludarabine (35.1% ± 17.4%) ($P < .001$) or dexamethasone (49.8% ± 19.1%) ($P = .02$) alone. As shown below, drug-induced apoptosis involved mitochondrial alterations, including a loss of $\Delta\Psi_m$, generation of ROS, and cytochrome c release. Moreover, the caspase cascade was activated, as determined by the detection of the active form of caspase-3 and the proteolytic cleavage of PARP, an endogenous substrate of caspases.

Involvement of Bax on drug-induced apoptosis was analyzed in cells from all patients by means of an antibody directed against the NH_2-terminal region of Bax (clone YTH-6A7). This region is occluded in unstressed intact cells and hence is not available for binding by Bax NH_2-terminal epitope-specific antibodies.[24,25] Few untreated cells were stained with this antibody (17.6% ± 10.9%). An increase in the number of Bax-positive cells was observed following incubation with fludarabine (26.1% ± 14.4%), dexamethasone (37.7% ± 21.7%), or FCM (51.5% ± 25.1%) ($P < .001$ in all cases). Figure 1A shows annexin V binding and Bax staining from one representative case. In drug-treated cells, a cluster of cells with Bax-associated fluorescence was observed. The number of both spontaneous and drug-induced apoptotic cells directly correlated with the number of Bax-positive cells ($r = 0.836$; $P < .001$) (Figure 1B).

Similar results were obtained with the use of other antibodies directed against the NH_2-terminal epitopes of Bax (Δ21 and N20 from Santa Cruz Biotechnology, and polyclonal anti-Bax from Upstate Biotechnology). On the contrary, when antibodies directed against amino acids 43 through 61 were used, no differences in the fluorescence pattern between control and drug-treated CLL cells were observed (data not shown).

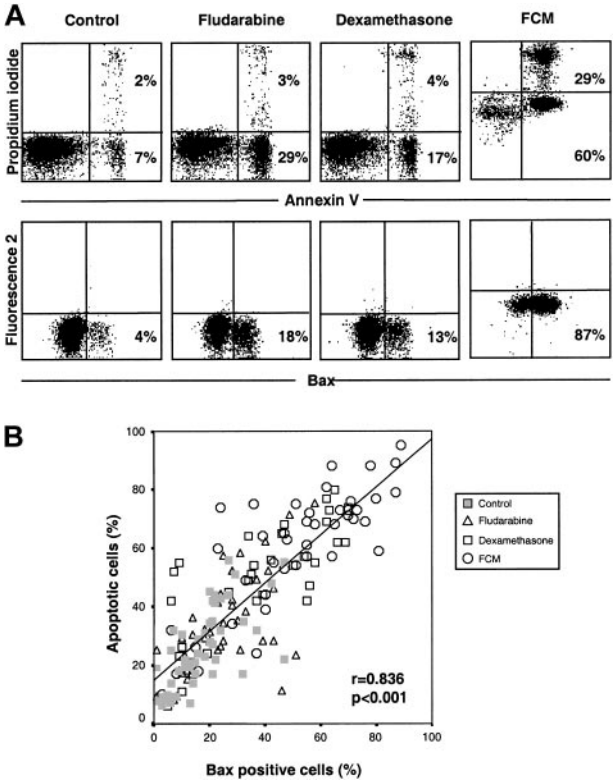

Figure 1. Drug-induced apoptosis is accompanied by conformational changes in Bax. (A) Cells from a representative CLL patient were incubated in the presence or absence of 5 μg/mL fludarabine, 10 μM dexamethasone, or the FCM combination for 24 hours. Bax conformational changes were determined by staining with anti-Bax (clone YHT-6A7) and flow cytometric analysis. Cell viability was quantified by annexin V binding. In FCM-treated cells, a shift in the signal of fluorescence 2 (585 nm) and 3 (630 nm) was observed owing to the incorporation of mitoxantrone. The percentage of positive cells is indicated in each panel. (B) Correlation between cell viability and Bax-positive cells following incubation with medium alone, fludarabine, dexamethasone, or the FCM combination in cells from 33 CLL patients.

Bax conformational changes precede caspase activation in drug-induced apoptosis

To establish whether the changes in Bax conformation preceded or followed caspase activation, cells from 8 patients were preincubated in the presence or absence of 200 μM Z-VAD.fmk prior to the addition of FCM. As seen in Figure 2, the inhibition of the caspase pathway reversed FCM-induced phosphatidylserine exposure, ROS generation, caspase-3 activation, and PARP proteolysis (data not shown). Loss of $\Delta\Psi_m$ was partially reversed by inhibition of caspases. In contrast, Bax conformational changes were observed despite inhibition of the caspase cascade. Similar results were obtained with fludarabine or dexamethasone alone (data not shown). These results place the conformational changes of Bax upstream of the caspase activation or in a caspase-independent manner.

Analysis of apoptosis-related proteins during drug-induced apoptosis in CLL

After FCM incubation, no changes in the overall protein levels of Bax, Bak, and Bcl-2 were detected, whereas down-regulation of Mcl-1, up-regulation of p53, and proteolysis of PARP were observed (Figure 3A). The cellular localization of Bcl-2 family proteins (Bax, Bcl-2, Bak, and Mcl-1) was analyzed by Western blot in mitochondrial and cytosolic protein fractions. As shown in Figure 3B, in untreated CLL cells, Bcl-2, Mcl-1, and Bak were present only in the mitochondrial fraction, whereas Bax was found predominantly in this fraction, but was also detected in the cytosolic fraction. Incubation with FCM induced a shift in the cellular localization of Bax from the cytosolic to the mitochondrial fraction, as well as a decrease in the levels of Mcl-1.

To assess if these proteins were integrated or only attached to mitochondria, mitochondrial fractions from untreated and FCM-treated cells were incubated with Na_2CO_3 to remove proteins attached to mitochondria (Figure 3B). In untreated CLL cells, Bak and Bcl-2 were detected only in the pellet of alkali-treated mitochondria, corresponding to proteins integrated into the mitochondria, whereas Bax and Mcl-1 were also detected in the alkali supernatant. Interestingly, in FCM-treated cells, Bax was found only in the pellet of alkali-treated mitochondria; this suggests that Bax had been integrated into mitochondria.

These results were corroborated by visualization of immunostaining with anti-Bax (clone YHT-6A7) (Figure 4). In untreated CLL cells, no staining with this monoclonal antibody was observed, whereas upon FCM treatment a clear punctuate staining was detected, indicating that a conformational change of Bax had been induced. This pattern indicated that Bax had a mitochondrial

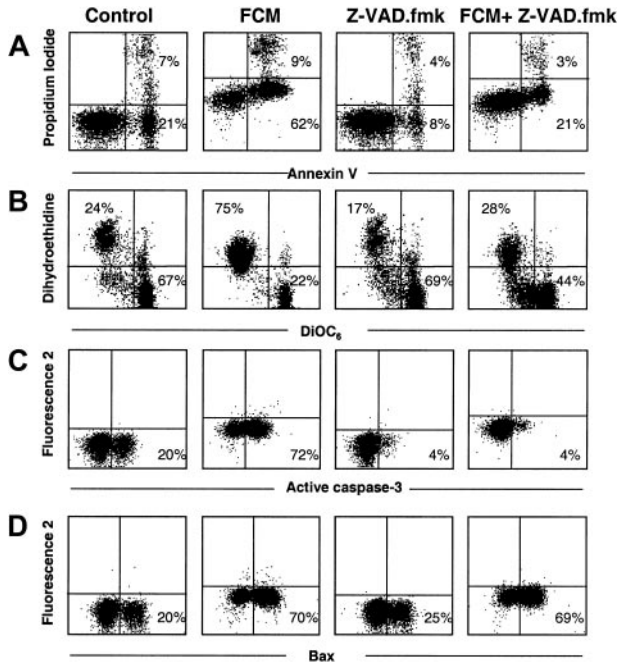

Figure 2. Conformational changes of Bax during drug-induced apoptosis precede caspase activation. Cells from a representative CLL patient were incubated with medium alone or the FCM combination in the presence or absence of 200 μM Z-VAD.fmk for 24 hours. Z-VAD.fmk was preincubated for 1 hour prior to the addition of FCM. In FCM-treated cells, a shift in the signal of fluorescence 2 (585 nm) and 3 (630 nm) was observed owing to the incorporation of mitoxantrone. The percentage of positive cells is indicated. Flow cytometric dot plots show cell viability as determined by annexin V binding (panel A); loss of $\Delta\Psi_m$ and ROS generation by dual staining with $DiOC_6$[3] and DHE (panel B); quantification of the active form of caspase-3 (panel C); and conformational changes of Bax as determined by staining with anti-Bax (clone YHT-6A7) (panel D).

localization in drug-treated cells, which was confirmed by simultaneous staining with Bcl-2 (data not shown). In addition, a double staining with Bax and cytochrome c was performed. As seen in the right panels of Figure 4, an intense and punctuated staining for cytochrome c was observed in untreated cells, where cytochrome c remained intact in the mitochondria. In contrast, in FCM-treated cells, a weak and diffuse cytochrome c staining was observed, suggesting that this protein had been released from mitochondria. Interestingly, in both control and FCM-treated cells, double staining confirmed that cells that had lost cytochrome c staining corresponded to those in which Bax had undergone conformational changes. Loss of cytochrome c was also observed by flow cytometry and confirmed by Western blot of cytosolic and mitochondrial fractions (Figure 5).

Bak underwent conformational changes during drug-induced apoptosis and correlated with Bax

Cells from 10 CLL patients were incubated with fludarabine, dexamethasone, or FCM for 24 hours and labeled with antibodies directed against the NH_2-terminal region of Bak (Ab-1 and 2-14 antibodies). As seen in Figure 6A, cells undergoing apoptosis showed a positive staining, which directly correlated with the degree of apoptosis ($r = 0.948$, $P < .001$) (Figure 6B), as well as with the number of Bax-positive cells ($r = 0.905$, $P < .001$) (Figure 6C).

As observed with Bax protein, preincubation of cells from 4 CLL patients with Z-VAD.fmk did not prevent Bak conformational change, whereas all the other cellular features of apoptosis were completely reversed, except for loss of $\Delta\Psi_m$, which was only partially reversed (data not shown).

Conformational changes of Bax and Bak are independent of p53 activation

It has been reported that Bax and Bak are regulated by p53 protein.[26,27] For this reason, p53 stabilization during drug-induced apoptosis was analyzed in cells from 13 CLL patients, either by flow cytometry or by Western blot (Figure 7A-B). Stabilization of p53 was detected following in vitro treatment with fludarabine or FCM in all cases analyzed. However, no activation of p53 protein was observed in any case after treatment with dexamethasone, although conformational changes of Bax and Bak were observed. Preincubation of cells with Z-VAD.fmk did not prevent stabilization of p53 protein (Figure 7B). These results suggest that p53 stabilization is not essential for conformational changes of Bax and Bak and precedes caspase activation.

Localization of p53 was analyzed on cytosolic and mitochondrial fractions. No protein was observed in cytosolic fractions of either untreated or treated cells, or in mitochondrial fractions of untreated cells. Interestingly, p53 was detected in mitochondrial fractions of FCM-treated cells and remained in this fraction following treatment with alkali (Figure 7C).

Discussion

In the present study, we have investigated the subcellular localization and the translocation of Bax and Bak, 2 proapoptotic members of the Bcl-2 family, in CLL cells after drug-induced apoptosis. This study shows, for the first time, that treatment of primary CLL cells with either dexamethasone, fludarabine, or FCM induce conformational changes of Bax and Bak that precede cell death.

Bax is a member of the Bcl-2 family of proteins that participates in the induction of apoptosis in response to a variety of apoptotic stimuli.[28] We and others have previously shown that the overall Bax protein levels are not altered during fludarabine- or FCM-induced apoptosis in CLL cells,[7,18] in contrast to other cell types.[29,30] In this study, we demonstrate that Bax conformational change is one of the first steps in drug-induced apoptosis in CLL cells and that it is accompanied by the characteristic features of the mitochondrial-dependent apoptosis pathway. Conformational changes of Bax were not blocked by the presence of the broad

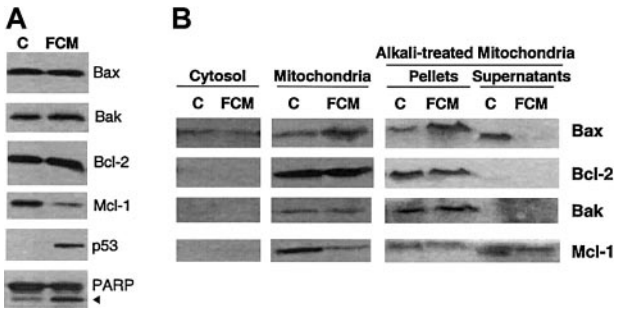

Figure 3. Apoptosis-related proteins during drug-induced cell death. (A) Whole-cell lysates were obtained from 2×10^6 cells from a representative CLL patient incubated in the absence (C) or presence of the FCM combination for 24 hours, and analyzed by Western blot. (B) Cytosolic and mitochondrial fractions were obtained from 50×10^6 cells incubated in the absence (C) or presence of the FCM combination for 24 hours. Mitochondrial fractions were either untreated or treated with alkali. All fractions were analyzed by Western blot. The position of the proteolytic fragment (85 kd) of PARP is indicated by an arrow.

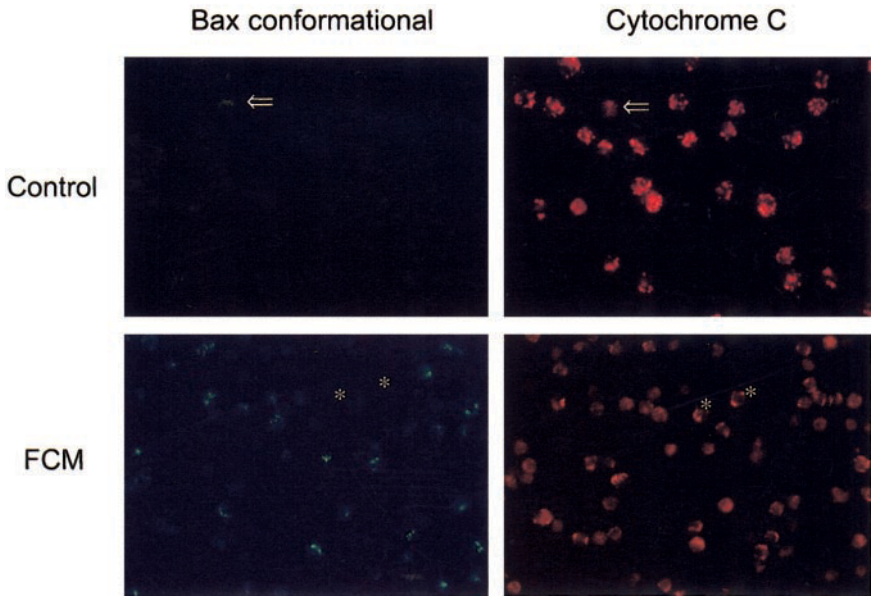

Figure 4. Cellular localization of Bax and cytochrome c during drug-induced apoptosis. Cells from a representative patient were incubated in the absence or presence of the FCM combination for 24 hours. Cells were immunostained with anti-Bax (clone YHT-6A7, green fluorescence) and anti–cytochrome c (red fluorescence). Photographs of the same fields were obtained with optical filters specific for green and red light (original magnifications, × 600). Arrows indicate the same apoptotic cell showing a punctuated Bax staining and having lost cytochrome c. Asterisks on the lower panel indicate viable cells (negative staining for Bax and bright punctuated signal for cytochrome c).

caspase inhibitor Z-VAD.fmk, indicating that Bax translocation precedes caspase activation or is caspase independent, as previously observed in some experimental models using cell lines.[25,31] The loss of $\Delta\Psi_m$ is only partially reversed by Z-VAD.fmk, suggesting that an initial loss of $\Delta\Psi_m$ is independent of caspases and may be due to integration of Bax into the outer mitochondrial membrane. In fact, recombinant Bax is able to form ion channels in artificial membranes.[32]

Previous studies showed that Bax is a cytosolic protein in healthy cells, unless it is loosely attached to the mitochondria. Upon induction of apoptosis, Bax translocates to mitochondria[11,33] and undergoes a conformational change that unmasks both the amino and the hydrophobic portion of the carboxyterminus; the latter being important for its proapoptotic function.[11,34] This translocation is followed by the insertion of Bax into the outer mitochondrial membrane, becoming an integral membrane protein. Our results show that although Bax is detected in the mitochondrial fraction of both treated and untreated CLL cells, Bax is inserted only into the mitochondrial membranes and becomes an integral mitochondrial protein after FCM treatment. This is in agreement with previous reports showing that the association of Bax with mitochondrial membranes changes from a weak to a strong insertion following apoptosis triggering.[35]

Bak is another proapoptotic member of the Bcl-2 family and shows high homology to Bax in size, sequence and biological activity.[9] Recently, a role for Bak in the mechanism of releasing mitochondrial intermembrane proteins in human leukemic cell lines in response to cytotoxic drugs has been described.[22] Indeed, it has been reported that Bak-deficient Jurkat cells are resistant to apoptosis.[36] Our results demonstrate that in primary CLL cells a conformational change of Bak is observed after genotoxic and nongenotoxic (dexamethasone) drug-induced apoptosis. In contrast to Bax, Bak is an integral mitochondrial protein in healthy cells, and modifications in this protein following apoptosis triggering can only be detected, as in the present study, by exposure of its amino-terminal region. The conformational changes of Bak also

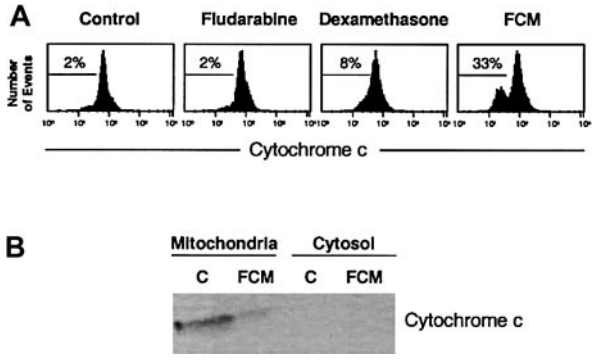

Figure 5. Analysis of cytochrome c in drug-induced apoptosis. (A) Flow cytometric analysis of cytochrome c staining. Cells from a representative CLL patient were incubated in the presence or absence of 5 μg/mL fludarabine, 10 μM dexamethasone, or the FCM combination for 24 hours, stained with anti–cytochrome c, and analyzed by flow cytometry. The percentage of cytochrome c–negative cells is indicated in each histogram. (B) Western blot of cytochrome c in mitochondrial and cytosolic fractions obtained from 50×10^6 cells of a representative CLL patient incubated in the presence or absence of FCM for 24 hours.

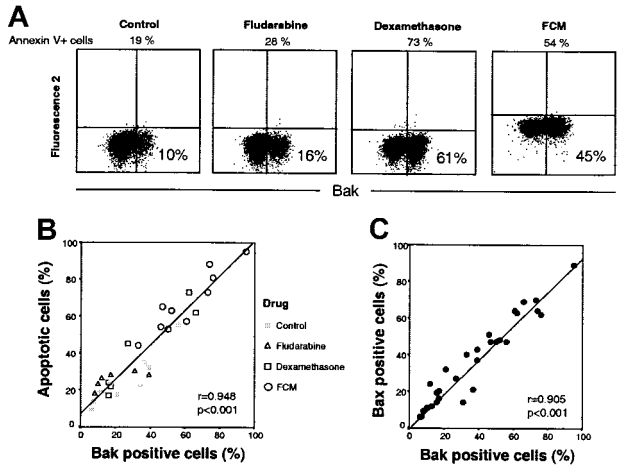

Figure 6. Bak conformational changes in drug-induced apoptosis of CLL cells. (A) Dot plots of Bak conformational changes in cells from one representative patient following incubation with medium alone, 5 μg/mL fludarabine, 10 μM dexamethasone, or the FCM combination for 24 hours. The percentage of Baκ-positive cells is indicated in each panel. (B) Correlation between cell viability and Bak-positive cells following incubation of cells from 10 patients with medium alone, fludarabine, dexamethasone, or the FCM combination. (C) Correlation of Bax and Baκ-positive cells following incubation of cells from 10 patients with medium alone, fludarabine, dexamethasone, or the FCM combination for 24 hours.

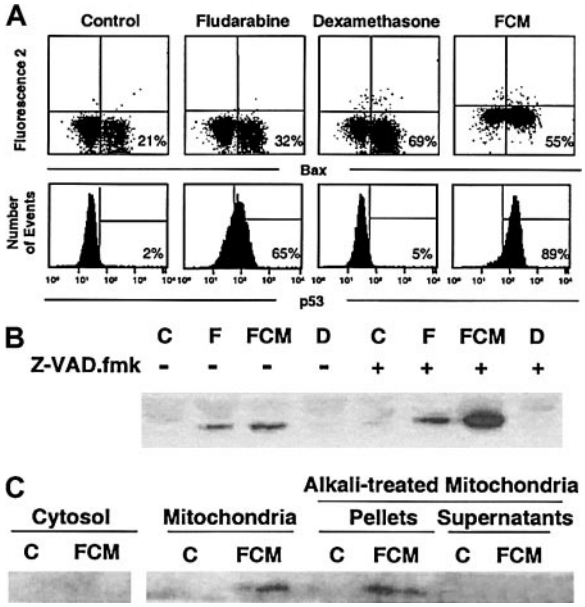

Figure 7. Activation of p53 is independent of Bax conformational changes. (A) Flow cytometric analysis of conformational changes of Bax and p53 activation in cells from a representative CLL patient incubated with medium alone or in the presence of 5 μg/mL fludarabine, 10 μM dexamethasone, or the FCM combination. (B) Western blot analysis of p53 protein. Whole-cell lysates were obtained from 2×10^6 cells from a representative CLL patient incubated with medium alone (C), fludarabine (F), FCM, or dexamethasone (D), in the presence (+) or absence (−) of 200 μM Z-VAD.fmk for 24 hours, and were analyzed by Western blot. (C) Cytosolic and mitochondrial fractions were obtained from 50×10^6 cells incubated in the absence (C) or presence of the FCM combination for 24 hours. Mitochondrial fractions were either left untreated or treated with alkali. All fractions were analyzed by Western blot.

occurred before caspase activation and directly correlated with the number of apoptotic cells and the number of Bax-positive cells. The conformational changes of these proteins are supposed to modify the protein-protein interactions that seem to be important for the integration of damage signals and the commitment of the cell to apoptotic death.[13]

Mitochondrial apoptosis signaling requires either Bak, which usually resides in mitochondria, or Bax, which translocates to mitochondria after apoptosis triggering. Furthermore, the coexistence of Bax and Bak in cells provides a redundancy in the apoptotic signaling pathway. In CLL cells, in contrast to other models using cell lines,[37,38] activation of apoptosis by different stimuli simultaneously activates conformational changes of both Bax and Bak proteins. Recently, a coalescence of both Bax and Bak in clusters adjacent to the mitochondrial membrane has been observed,[39] and its formation seems essential for cell death. Also, it has been shown that cells lacking both Bax and Bak, but not cells lacking one of these proteins, are resistant to multiple apoptotic stimuli, as well as to truncated Bid (tBid)–induced cytochrome c release and apoptosis.[36]

The apoptotic signals upstream of Bax and Bak are not completely known. Although it has been suggested that an increase in intracellular pH, occurring in the cytosol of cells undergoing apoptosis, induces a structural modification of cytosolic Bax followed by its translocation to the mitochondria,[40] the nuclear magnetic resonance spectroscopy of Bax protein demonstrates the absence of conformational changes of Bax at a pH ranging from 6 to 8.[34] Moreover, although it has been shown that the Na^+/H^+ exchange activity is drastically decreased in CLL cells in comparison with normal B cells,[41,42] conformational changes of Bax are also observed in normal B cells (data not shown).

The binding of cell death receptors by their ligands activates procaspase 8, which, in turn, truncates Bid (tBid). This truncated protein translocates to mitochondria where it binds directly to Bax or Bak, leading to a conformational change of these proteins.[10,36] Nevertheless, conformational changes of Bax and Bak are also observed in the absence of tBid.[36] Other proteins, such as p53, MEKK1, and c-myc, have also been described as upstream regulators of Bax and Bak conformation.[27,37,43,44] We have previously shown that fludarabine and the FCM combination induce the stabilization of p53 protein,[7] whereas this phenomenon is not observed in dexamethasone-treated CLL cells. In our model, Bax and Bak conformational changes occurred in response to both p53-dependent and p53-independent cytotoxic drugs, indicating that p53 is not required to execute the apoptotic program. Furthermore, our results also suggest that p53 is translocated and integrated into mitochondria following in vitro treatment with FCM. These results are in accord with previous studies describing this shift in the localization of p53 after drug treatment.[45]

Bcl-2 family members are the cellular gatekeepers of cell survival or death. A complex regulation of its members, not completely understood, has been proposed. Although Bax and Bak act as redundant proteins, specific regulation for each protein, as well as a differential response to apoptotic stimuli with a predominant use of Bax or Bak in the cell death process has been described.[37,46] The regulatory mechanisms proposed include post-transcriptional regulation, phosphorylation, dimerization, and protein displacement.[10] Therefore, the effect of these mechanisms, in addition to overall protein levels and ratios between proapoptotic and antiapoptotic members, should be taken into account when analyzing the role of these proteins as prognostic factors.

In summary, this study demonstrates that Bax and Bak, 2 proapoptotic members of the Bcl-2 family, undergo conformational changes in CLL cells in response to drug-induced apoptosis. These conformational changes precede mitochondrial dysfunction and caspase activation and are independent of p53 activation. The conformational changes of Bax and Bak directly correlate with cell death, suggesting an implication of both proteins in the apoptotic pathway of CLL cells.

References

1. Rozman C, Montserrat E. Chronic lymphocytic leukemia. N Engl J Med. 1995;333:1052-1057.
2. Reed JC. Molecular biology of chronic lymphocytic leukemia. Semin Oncol. 1998;25:11-18.
3. Byrd JC, Waselenko JK, Keating M, Rai K, Grever MR. Novel therapies for chronic lymphocytic leukemia in the 21st century. Semin Oncol. 2000;27:587-597.
4. Robertson LE, Chubb S, Meyn RE, et al. Induction of apoptotic cell death in chronic lymphocytic leukemia by 2-chloro-2′-deoxyadenosine and 9-beta-D-arabinosyl-2-fluoroadenine. Blood. 1993;81:143-150.
5. Begleiter A, Lee K, Israels LG, Mowat MR, Johnston JB. Chlorambucil induced apoptosis in chronic lymphocytic leukemia (CLL) and its relationship to clinical efficacy. Leukemia. 1994;8(suppl 1):S103-S106.
6. McConkey DJ, Aguilar-Santelises M, Hartzell P, et al. Induction of DNA fragmentation in chronic B-lymphocytic leukemia cells. J Immunol. 1991; 146:1072-1076.
7. Bellosillo B, Villamor N, Colomer D, Pons G, Montserrat E, Gil J. In vitro evaluation of fludarabine in combination with cyclophosphamide and/or mitoxantrone in B-cell chronic lymphocytic leukemia. Blood. 1999;94:2836-2843.
8. Herr I, Debatin KM. Cellular stress response and apoptosis in cancer therapy. Blood. 2001;98: 2603-2614.
9. Adams JM, Cory S. Life-or-death decisions by the Bcl-2 protein family. Trends Biochem Sci. 2001; 26:61-66.
10. Gross A, McDonnell JM, Korsmeyer SJ. BCL-2 family members and the mitochondria in apoptosis. Genes Dev. 1999;13:1899-1911.
11. Gross A, Jockel J, Wei MC, Korsmeyer SJ. Enforced dimerization of BAX results in its translocation, mitochondrial dysfunction and apoptosis. EMBO J. 1998;17:3878-3885.

12. Nechushtan A, Smith CL, Hsu YT, Youle RJ. Conformation of the Bax C-terminus regulates subcellular location and cell death. EMBO J. 1999;18: 2330-2341.
13. Griffiths GJ, Dubrez L, Morgan CP, et al. Cell damage-induced conformational changes of the pro-apoptotic protein Bak in vivo precede the onset of apoptosis. J Cell Biol. 1999;144:903-914.
14. Hanada M, Delia D, Aiello A, Stadtmauer E, Reed JC. bcl-2 gene hypomethylation and high-level expression in B-cell chronic lymphocytic leukemia. Blood. 1993;82:1820-1828.
15. Robertson LE, Plunkett W, McConnell K, Keating MJ, McDonnell TJ. Bcl-2 expression in chronic lymphocytic leukemia and its correlation with the induction of apoptosis and clinical outcome. Leukemia. 1996;10:456-459.
16. Pepper C, Bentley P, Hoy T. Regulation of clinical chemoresistance by bcl-2 and bax oncoproteins in B-cell chronic lymphocytic leukaemia. Br J Haematol. 1996;95:513-517.
17. Pepper C, Hoy T, Bentley DP. Bcl-2/Bax ratios in chronic lymphocytic leukaemia and their correlation with in vitro apoptosis and clinical resistance. Br J Cancer. 1997;76:935-938.
18. Kitada S, Andersen J, Akar S, et al. Expression of apoptosis-regulating proteins in chronic lymphocytic leukemia: correlations with in vitro and in vivo chemoresponses. Blood. 1998;91:3379-3389.
19. Pepper C, Thomas A, Hoy T, Fegan C, Bentley P. Flavopiridol circumvents Bcl-2 family mediated inhibition of apoptosis and drug resistance in B-cell chronic lymphocytic leukaemia. Br J Haematol. 2001;114:70-77.
20. Jaffe ES, Harris NL, Stein H, Vardiman JWE, eds. World Health Organization Classification of Tumours: Pathology and Genetics of Tumours of Haematopoietic and Lymphoid Tissues. Lyon, France: IARC Press; 2001.
21. Bellosillo B, Villamor N, Lopez-Guillermo A, et al. Complement-mediated cell death induced by rituximab in B-cell lymphoproliferative disorders is mediated in vitro by a caspase-independent mechanism involving the generation of reactive oxygen species. Blood. 2001;98:2771-2777.
22. Wang GQ, Gastman BR, Wieckowski E, et al. A role for mitochondrial Bak in apoptotic response to anticancer drugs. J Biol Chem. 2001;276: 34307-34317.
23. Bellosillo B, Dalmau M, Colomer D, Gil J. Involvement of CED-3/ICE proteases in the apoptosis of B-chronic lymphocytic leukemia cells. Blood. 1997;89:3378-3384.
24. Hsu YT, Youle RJ. Bax in murine thymus is a soluble monomeric protein that displays differential detergent-induced conformations. J Biol Chem. 1998;273:10777-10783.
25. Desagher S, Osen-Sand A, Nichols A, et al. Bid-induced conformational change of Bax is responsible for mitochondrial cytochrome c release during apoptosis. J Cell Biol. 1999;144:891-901.
26. Pearson AS, Spitz FR, Swisher SG, et al. Up-regulation of the proapoptotic mediators Bax and Bak after adenovirus-mediated p53 gene transfer in lung cancer cells. Clin Cancer Res. 2000;6: 887-890.
27. Miyashita T, Reed JC. Tumor suppressor p53 is a direct transcriptional activator of the human bax gene. Cell. 1995;80:293-299.
28. Knudson CM, Korsmeyer SJ. Bcl-2 and Bax function independently to regulate cell death. Nat Genet. 1997;16:358-363.
29. Schuler M, Bossy-Wetzel E, Goldstein JC, Fitzgerald P, Green DR. p53 induces apoptosis by caspase activation through mitochondrial cytochrome c release. J Biol Chem. 2000;275:7337-7342.
30. Zhou XM, Wong BC, Fan XM, et al. Non-steroidal anti-inflammatory drugs induce apoptosis in gastric cancer cells through up-regulation of bax and bak. Carcinogenesis. 2001;22:1393-1397.
31. Gilmore AP, Metcalfe AD, Romer LH, Streuli CH. Integrin-mediated survival signals regulate the apoptotic function of Bax through its conformation and subcellular localization. J Cell Biol. 2000;149: 431-446.
32. Bernardi P, Broekemeier KM, Pfeiffer DR. Recent progress on regulation of the mitochondrial permeability transition pore; a cyclosporin-sensitive pore in the inner mitochondrial membrane. J Bioenerg Biomembr. 1994;26:509-517.
33. Hsu YT, Wolter KG, Youle RJ. Cytosol-to-membrane redistribution of Bax and Bcl-X(L) during apoptosis. Proc Natl Acad Sci U S A. 1997;94: 3668-3672.
34. Suzuki M, Youle RJ, Tjandra N. Structure of Bax: coregulation of dimer formation and intracellular localization. Cell. 2000;103:645-654.
35. Goping IS, Gross A, Lavoie JN, et al. Regulated targeting of BAX to mitochondria. J Cell Biol. 1998;143:207-215.
36. Wei MC, Zong WX, Cheng EH, et al. Proapoptotic BAX and BAK: a requisite gateway to mitochondrial dysfunction and death. Science. 2001;292: 727-730.
37. Mandic A, Viktorsson K, Molin M, et al. Cisplatin induces the proapoptotic conformation of Bak in a deltaMEKK1-dependent manner. Mol Cell Biol. 2001;21:3684-3691.
38. Wang GQ, Wieckowski E, Goldstein LA, et al. Resistance to granzyme B-mediated cytochrome c release in Bak-deficient cells. J Exp Med. 2001; 194:1325-1337.
39. Nechushtan A, Smith CL, Lamensdorf I, Yoon SH, Youle RJ. Bax and Bak coalesce into novel mitochondria-associated clusters during apoptosis. J Cell Biol. 2001;153:1265-1276.
40. Khaled AR, Kim K, Hofmeister R, Muegge K, Durum SK. Withdrawal of IL-7 induces Bax translocation from cytosol to mitochondria through a rise in intracellular pH. Proc Natl Acad Sci U S A. 1999;96:14476-14481.
41. Ghigo D, Gaidano G, Treves S, et al. Na+/H+ antiporter has different properties in human B lymphocytes according to CD5 expression and malignant phenotype. Eur J Immunol. 1991;21: 583-588.
42. Gaidano G, Ghigo D, Schena M, et al. Na+/H+ exchange activation mediates the lipopolysaccharide-induced proliferation of human B lymphocytes and is impaired in malignant B-chronic lymphocytic leukemia lymphocytes. J Immunol. 1989;142:913-918.
43. Mitchell KO, Ricci MS, Miyashita T, et al. Bax is a transcriptional target and mediator of c-myc-induced apoptosis. Cancer Res. 2000;60:6318-6325.
44. Kannan K, Amariglio N, Rechavi G, et al. DNA microarrays identification of primary and secondary target genes regulated by p53. Oncogene. 2001;20:2225-2234.
45. Marchenko ND, Zaika A, Moll UM. Death signal-induced localization of p53 protein to mitochondria: a potential role in apoptotic signaling. J Biol Chem. 2000;275:16202-16212.
46. Ke N, Godzik A, Reed JC. Bcl-B, a novel Bcl-2 family member that differentially binds and regulates Bax and Bak. J Biol Chem. 2001;276: 12481-12484.

Complement-mediated cell death induced by rituximab in B-cell lymphoproliferative disorders is mediated in vitro by a caspase-independent mechanism involving the generation of reactive oxygen species

Beatriz Bellosillo, Neus Villamor, Armando López-Guillermo, Silvia Marcé, Jordi Esteve, Elias Campo, Dolors Colomer, and Emili Montserrat

Mechanisms involving the in vitro effect of rituximab in cells from 55 patients with B-cell lymphoproliferative disorders were investigated. No cytotoxic effect was observed when cells were incubated with rituximab alone, but in the presence of human AB serum rituximab induced complement-dependent cell death (R-CDC). A cytotoxic effect was observed in cells from 9 of 33 patients with B-cell chronic lymphocytic leukemia, 16 of 16 patients with mantle-cell lymphoma, 4 of 4 patients with follicular lymphoma, and 2 of 2 patients with hairy-cell leukemia. R-CDC was observed in cells from patients expressing more than 50×10^3 CD20 molecules per cell, and directly correlated with the number of CD20 molecules per cell. Preincubation with anti-CD59 increased the cytotoxic effect of rituximab and sensitized cells from non-sensitive cases. Neither cleavage of poly-ADP ribose polymerase (PARP) nor activation of caspase-3 was observed in R-CDC. In addition, no cells with a hypodiploid DNA content were detected and R-CDC was not prevented by a broad-spectrum caspase inhibitor, suggesting a caspase-independent mechanism. Incubation with rituximab in the presence of AB serum induced a rapid and intense production of reactive oxygen species (ROS). R-CDC was blocked by the incubation of cells with N-acetyl-L-cysteine (NAC) or Tiron, 2 ROS scavengers, indicating that the cytotoxic effect was due to the generation of superoxide (O_2^-) radicals. In conclusion, the results of the present study suggest that CD20, CD59, and complement have a role in the in vitro cytotoxic effect of rituximab, which is mediated by a caspase-independent process that involves ROS generation. (Blood. 2001;98: 2771-2777)

Introduction

Rituximab is a chimeric monoclonal antibody directed against CD20, an antigen present both on normal B lymphocytes and on cells from most B-cell lymphoproliferative disorders.[1] Rituximab is currently employed in the treatment of follicular lymphoma (FL) either alone[2,3] or in combination with chemotherapy.[4] Moreover, there is an increasing interest in using rituximab in other $CD20^+$ B-cell lymphoproliferative disorders, such as mantle-cell lymphoma (MCL) or B-cell chronic lymphocytic leukemia (B-CLL).[5,6] A direct relationship between the clinical efficacy and the intensity of CD20 expression has been proposed, suggesting that patients with high CD20 expression are more likely to respond to rituximab.

The signaling pathways involved in the effect of rituximab are not clearly established. Recently, complement-mediated cell lysis has been proposed as the major and most-efficient effector mechanism of rituximab.[1,7] However, the signal transduction pathways activated by complement, which precede cell death, have not been fully determined. Moreover, in vitro studies performed in cell lines suggest that rituximab binding to CD20 could induce apoptosis, mainly through caspase activation,[8] but other pathways, such as activation of the Src-family kinases[9] and antibody-dependent cell-mediated cytotoxicity (ADCC),[1,7] have also been described.

Complement-mediated cell lysis involves a cascade activation of proteins leading to the formation of the membrane attack complex, which produces a direct lysis of the target cells. This lysis is regulated by membrane-bound regulatory proteins, among which CD55 and CD59 seem to be the most important. CD55 binds to C3b and C4b and accelerates the decay of C3 and C5 convertases, whereas CD59 binds to C8 and C9 and prevents pore formation by the membrane attack complex,[10] the final step of complement lysis. According to recent studies, these proteins could be implicated in the cytotoxic effect of rituximab.[7,11]

The aims of this study were to correlate the cytotoxic effect of rituximab with CD20 expression in a variety of $CD20^+$ B-cell lymphoid malignancies, and to analyze the signaling pathways

From the Hematopathology Unit, Department of Hematology, Institute of Hematology and Oncology, Department of Pathology, Postgraduate School of Hematology Farreras-Valentí; the Institut d'Investigacions Biomèdiques August Pi i Sunyer (IDIBAPS), Hospital Clínic; and the University of Barcelona, Barcelona, Spain.

Submitted January 18, 2001; accepted May 14, 2001.

Supported in part by research fellowships from the Instituto de Salud Carlos III (B.B.) and Fondo de Investigaciones Sanitarias (FIS) (S.M.); FIS grant numbers 98/0996, 99/0189, and 00/0946; José Carreras International Foundation Against Leukemia (EM/P-01 and CR/P-00); Roche España; and the Asociación Española Contra el Cáncer, Barcelona, Spain.

Roche Spain provides funds for research activities of the Institute of Hematology and Oncology.

B.B and N.V. contributed equally to this study. D.C. and E.M. share the senior authorship of this paper.

Reprints: Emili Montserrat, Institute of Hematology and Oncology, Department of Hematology, Hospital Clínic, Villarroel 170, 08036 Barcelona, Spain; e-mail: emontse@clinic.ub.es.

The publication costs of this article were defrayed in part by page charge payment. Therefore, and solely to indicate this fact, this article is hereby marked "advertisement" in accordance with 18 U.S.C. section 1734.

involved in complement-dependent cell death (CDC), focusing on complement regulatory proteins.

Patients, materials, and methods

Patients

Fifty-five patients (35 men and 20 women) with a median age of 64 years (range, 32 to 88 years) who were diagnosed with B-cell chronic lymphoproliferative disorders (33 B-CLL, 16 MCL, 4 FL, and 2 hairy-cell leukemia [HCL]) were included in the study. The diagnosis was established according to the World Health Organization classification.[12] Patients with B-CLL entering this study were selected according to CD20 expression in conventional flow cytometry. All patients were informed of the investigational nature of this study and informed consent was obtained from each patient in accordance with Hospital Clínic ethical committee guidelines.

Reagents

Rituximab was obtained from Roche (Hertfordshire, United Kingdom). 4,5-dihydroxy-1,3-benzene disulfonic (Tiron) was obtained from Sigma Chemical (St Louis, MO). N-benzyloxycarbonyl-Val-Ala-Asp-fluoromethyl ketone (Z-VAD.fmk) was obtained from Bachem (Bubendorf, Switzerland). N-acetyl-L-cysteine (NAC) and PP2 were purchased from Calbiochem-Novabiochem (La Jolla, CA). Antibodies against CD20 (Leu 16), CD19-phycoerythrin (PE) (Leu12), and CD3-PE (Leu 4) were obtained from Becton Dickinson (San Jose, CA); against CD59 (clone MEM 43) from CLB (Amsterdam, The Netherlands); and against CD55 (clone Bric216) from Serotec (Oxford, United Kingdom). Antibodies against CD59 (clone 193-27) and CD55 (clone 143-30) were kindly provided by Dr R. Vilella from the Immunology Department of the Hospital Clinic, Barcelona, Spain.

Isolation of cells

Mononuclear cells were isolated from peripheral blood samples by centrifugation on a Ficoll/Hypaque (Seromed, Berlin, Germany) gradient and cryopreserved in liquid nitrogen in the presence of 10% dimethyl sulfoxide (DMSO). Cells from 5 cases (1 B-CLL, 3 MCL, and 1 FL) were obtained from lymph node biopsy or spleen after repetitive infiltration with RPMI 1640 culture medium (GibcoBRL, Paisley, Scotland).

Cell culture

Lymphocytes were cultured immediately after thawing at a concentration of 5×10^6 cells/mL in RPMI 1640 culture medium supplemented with 10% heat inactivated fetal calf serum (BioWhittaker, Verviers, Belgium), 2 mM glutamine, and 0.04 mg/mL gentamicin at 37°C in a humidified atmosphere containing 5% carbon dioxide. Factors were added at the beginning of the culture.

Analysis of cell viability by annexin binding

Exposure of phosphatidylserine residues was quantified by surface annexin V staining as previously described.[13] Briefly, cells were washed in binding buffer (10 mM HEPES, pH 7.4, 2.5 mM $CaCl_2$, 140 mM NaCl), resuspended in 200 μL and incubated with 0.5 μg/mL annexin V–fluorescein isothiocyanate (FITC) (Bender Medsystems, Vienna, Austria) for 15 minutes in the dark. Cells were washed again and resuspended in binding buffer. A quantity of 5 μg/mL propidium iodide (PI) (Sigma Chemical) was added to each sample prior to flow cytometric analysis (FACScan; Becton Dickinson). Ten thousand cells were acquired per sample using CELLquest software and data were analyzed with the Paint-a-gate Pro software (Becton Dickinson). All experiments were performed in duplicate. In some experiments, cells were labeled simultaneously with annexin V–FITC and anti–CD3-PE, in order to separately analyze the cytotoxic effect on B and T lymphocytes.

Propidium iodide DNA staining

Quantification of apoptosis by PI staining and fluorescence-activated cell sorting (FACS) analysis was performed as previously described.[14] Briefly, cells were harvested and fixed in 70% ethanol. Cells were centrifuged, washed in phosphate-buffered saline (PBS) and resuspended in 0.5 mL PBS containing PI (5 μg/mL) and RNase (100μg/mL) (Boehringer Mannheim, Mannheim, Germany). Tubes were incubated for 30 minutes at 37°C and placed at 4°C in the dark overnight prior to flow cytometry analysis.

Assessment of mitochondrial transmembrane potential and reactive oxygen species production

Changes in mitochondrial transmembrane potential ($\Delta\Psi_m$) were evaluated by staining with 1 nM 3,3′-dihexyloxacarbocyanine iodide ($DiOC_6[3]$; Molecular Probes, Eugene, OR). Reactive oxygen species (ROS) production was determined by staining with 2 μM dihydroethidine (DHE; Molecular Probes). Cells were incubated with the dyes for 15 minutes at 37°C, washed, resuspended in PBS and analyzed by flow cytometry. A decrease in the signal of $DiOC_6[3]$ (FL1) was indicative of abnormalities in $\Delta\Psi_m$ and appearance of FL2 signal was indicative of ROS production. Ten thousand cells were acquired in a FACScan flow cytometer. All experiments were performed in duplicate.

Kinetic studies of ROS generation

Cells were preincubated for 5 minutes with 50 μg/mL rituximab, and cell acquisition in a FACScan was started after incubation with DHE for one minute. AB serum was added after the first minute of cell acquisition and ROS production was recorded for 15 minutes. Kinetics of ROS generation were analyzed using the free software WinMDI 2.8 version (http://archive.uwcm.ac.uk/uwcm/hg/hoy/software.html).

Flow cytometric detection of the active form of caspase-3

Cells were fixed and permeabilized using the Cytofix/Cytoperm kit (Pharmingen, San Diego, CA) for 20 minutes at 4°C, pelleted and washed with Perm/Wash buffer (Pharmingen). Cells were then stained with the polyclonal antibody against the active form of caspase-3 (Pharmingen) (0.25 μg/L $\times$ 10^6 cells) for 20 minutes at room temperature, washed in Perm/Wash buffer, stained with goat anti–rabbit-FITC (SuperTechs, Bethesda, MD), and analyzed in a FACScan.

Quantification of CD20, CD55, and CD59 membrane proteins

Cells from patients or healthy donors (n = 19) were incubated with saturating amounts of monoclonal antibodies against CD20 (Leu16), CD55 (143-30), and CD59 (MEM 43) for 45 minutes at 4°C, washed twice in PBS and incubated with goat anti–mouse-FITC (Dako, Globstrub, Denmark) in the same conditions. The beads of QIFKIT (Dako) were processed in parallel following the manufacturer's recommendations. The mean FL1 channel for every bead population was used to calculate a standard curve and the number of molecules per cell was obtained by interpolation of the mean FL1 channel value for each patient. To quantify the number of complement regulatory proteins on B cells, samples stained with CD55 and CD59 were subsequently incubated with normal mouse serum (Dako) for 5 minutes, followed by CD19-PE monoclonal antibody.

Western blot

Cells were lysed in 80 mM Tris HCl pH 6.8, 2% sodium dodecyl sulfate (SDS), 10% glycerol, 0.1 M dithiothreitol (DTT) and equal amounts of protein were separated by electrophoresis on 12% polyacrylamide gel and transferred to Immobilon-P (Millipore, Bedford, MA) membranes. The membranes were incubated with polyclonal antibody against poly-ADP ribose polymerase (PARP) (Boehringer Mannheim). Antibody binding was detected using a secondary antibody (mouse anti–rabbit immunoglobulin; Dako) conjugated to horseradish peroxidase and an enhanced chemiluminiscence (ECL) detection kit (Amersham, Buckinghamshire, United Kingdom).

Statistical analysis

A case was considered sensitive to rituximab when cell death assessed by exposure of phosphatidylserine residues was more than or equal to 15% of cell death observed in control cells. Comparison of CD20, CD55, and CD59 cell levels between healthy donors and patients, and between sensitive and nonsensitive cases were performed using the nonparametric Mann-Whitney test. The effect of blockage with anti-CD55 and/or anti-CD59 was analyzed by means of linear regression models with random effects using a panel data structure, adjusted by normalized values of CD55 and CD59 molecules per cell, with STATA Statistical Software, Release 6.0 (Stata, College Station, TX).

Results

Rituximab induces cell death of tumor B cells in the presence of complement

To analyze the in vitro effect of rituximab on the viability of tumor cells from patients with B-cell lymphoproliferative disorders, a dose-response study was first performed in cells from 3 patients. No cytotoxic effect was observed when cells were incubated with rituximab alone (with doses ranging from 10 to 100 μg/mL) for increasing periods of time (up to 5 days). However, when normal human AB serum (AB) was added as a source of complement, rituximab produced a cytotoxic effect after 24 hours of incubation. This effect was dose dependent for both rituximab and AB (with quantities ranging from 1% to 40%) and could be detected using doses as low as 10 μg/mL rituximab and 1% AB. A discriminant cytotoxic effect was observed with 50 μg/mL rituximab in the presence of 10% AB. Thus, this was the combination used in all subsequent experiments.

The cytotoxic effect of rituximab in the presence of AB (rituximab+AB) was characterized by a reduction in the forward scatter (FSC) and an increase in the side scatter (SSC), indicative of cell shrinkage (Figure 1A), as well as an exposure of phosphatidylserine residues, as shown by the increase in annexin V–labeled cells (Figure 1B), and loss of $\Delta\Psi_m$, determined by staining with $DiOC_6[3]$ (Figure 1C).

Inactivation of the complement by heating AB at 56°C for 30 minutes completely abolished the cytotoxic effect of rituximab.

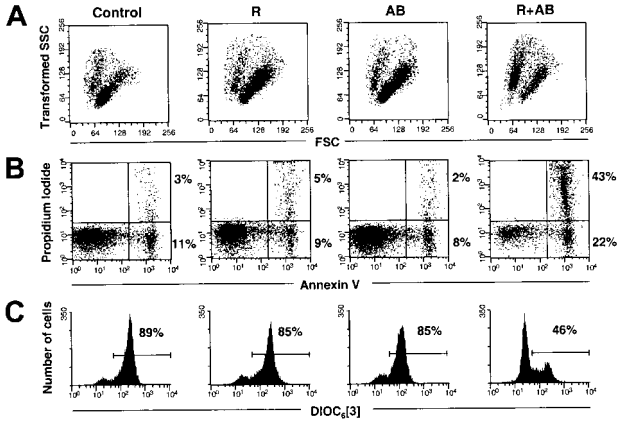

Figure 1. Cell death induction by the combination of rituximab and normal human AB serum. Cells from a representative $CD20^{++}$ patient with follicular lymphoma (FL) were incubated in the presence or absence of 50 μg/mL rituximab and 10% AB (R+AB) for 24 hours and analyzed by flow cytometry. (A) Flow cytometric plots showing FSC/SSC pattern. (B) Flow cytometric plots showing annexin V binding. (C) Histogram showing mitochondrial transmembrane potential after staining with $DiOC_6[3]$.

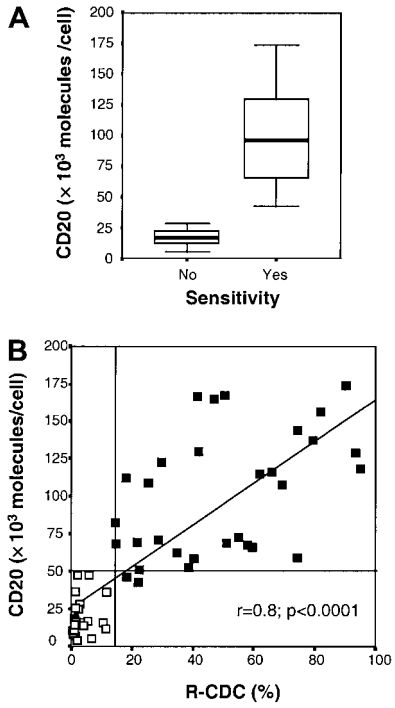

Figure 2. Relationship between CD20 expression and R-CDC. (A) Histograms of the mean values of the number of CD20 molecules per cell according to the sensitivity to rituximab+AB. (B) Correlation between the number of CD20 molecules per cell and the percentage of R-CDC obtained, in cells from nonsensitive (■) and sensitive (□) patients.

Incubation of cells with AB alone did not induce cell death but, to the contrary, produced a protective effect when compared with cells incubated with medium alone (data not shown).

The in vitro effect of rituximab+AB was analyzed on cells from 55 patients. In the above-mentioned conditions, R-CDC was observed in cells from 31 of the 55 patients (56%). The distribution of R-CDC among the different lymphoproliferative disorders was as follows: 9 of 33 in B-CLL (27%), 16 of 16 in MCL (100%), 4 of 4 in FL (100%), and 2 of 2 in HCL (100%).

R-CDC was not observed on $CD3^+$ cells from 20 cases as assessed by multiparametric flow cytometry analysis (data not shown), with this indicating that the cytotoxic effect of rituximab was restricted to B cells.

R-CDC depends on CD20 expression

In order to analyze the differences between cases that are sensitive (cytotoxicity ≥ 15%) and nonsensitive (cytotoxicity < 15%) to rituximab+AB, we quantified the expression of the CD20 antigen. As shown in Figure 2A, a significant difference ($P < .0001$) was found between the CD20 mean values of sensitive cases ($100.7 \pm 41 \times 10^3$ molecules per cell; n = 31) and nonsensitive cases ($18.7 \pm 12 \times 10^3$ molecules per cell; n = 24). All the cases expressing more than or equal to 50×10^3 molecules of the CD20 antigen on the cell membrane surface ($CD20^{++}$) (n = 29) showed R-CDC, whereas no cytotoxic effect was observed in cases with CD20 levels less than 40×10^3 molecules per cell ($CD20^{dim}$) (n = 22). Interestingly, a direct correlation was found between R-CDC and the number of CD20 molecules per cell (r = 0.8, $P < .0001$) (Figure 2B).

No modifications were observed in the FSC/SSC pattern or in annexin V binding when cells from 4 $CD20^{dim}$ cases were

Table 1. Quantification of the expression of CD20, CD55, and CD59 in cells from patients with B-lymphoproliferative disorders and healthy donors

	n	Molecules/cell ($\times 10^3$)		
		CD20	CD55	CD59
B-CLL	33	31.9 ± 26*	9.7 ± 4*	12.1 ± 6
Nonsensitive	24	18.7 ± 12*	9.4 ± 5*	12.8 ± 7
Sensitive**	9	67.0 ± 20	10.4 ± 4*	10.3 ± 6
MCL	16	113.2 ± 39	11.9 ± 5	9.0 ± 6
FL	4	96.0 ± 38	10.3 ± 4	16.5 ± 10
HCL	2	162.2 ± 7	2.1 ± 1	9.8 ± 11
Healthy donors	19	94.9 ± 37	13.6 ± 29	12.2 ± 4

*$P < .02$ versus healthy donors.
**$P < .001$ sensitive B-CLL versus nonsensitive B-CLL.

incubated with rituximab+AB for longer periods of time (up to 5 days) (data not shown).

As shown in Table 1, the number of CD20 molecules was significantly lower in B-CLL cells than in normal B cells, whereas no difference was observed in the other types of B-lymphoproliferative disorders analyzed. Of note, cells from nonsensitive B-CLL cases had significantly lower CD20 levels than cells from sensitive B-CLL cases.

Regulation of R-CDC by CD55 and CD59

To study the role of the complement in R-CDC, we quantified the expression of CD55 and CD59, 2 complement regulatory proteins. The number of CD55 molecules per cell was significantly lower in B-CLL and HCL cells than in normal B cells, whereas no difference was observed in other B-lymphoproliferative disorders (Table 1). Regarding the number of CD59 molecules, only the subgroup of sensitive B-CLL cells expressed lower CD59 molecules per cell than normal B cells. No correlation was found between R-CDC and the number of CD55 or CD59 molecules on the cell surface. Among 4 B-CLL samples that expressed between 40×10^3 molecules per cell and 50×10^3 CD20 molecules per cell ($CD20^+$), only 2 of them were sensitive to rituximab. Interestingly, these 2 cases expressed lower CD59 levels than the 2 nonsensitive cases (Figure 3A).

To better understand the role of CD55 and CD59, the effect of rituximab+AB was analyzed in the presence of anti-CD59 and/or anti-CD55 in cells from 9 B-CLL patients (Figure 3B). No cytotoxic effect was observed when cells were incubated with these monoclonal antibodies alone, or combined with AB, indicating that they cannot activate the complement by themselves. The statistical analysis of the mean values obtained for these 9 patients showed that the viability of cells incubated with rituximab+AB was 80 ± 7% (95% confidence interval [CI]: 67-93). The addition of anti-CD59 produced a significant decrease in cell viability by 48 units (95% CI: 38-57; $P < .001$), whereas addition of anti-CD55 only produced a decrease of 8 units (95% CI: 0-17; $P = .078$). The combination of the 2 monoclonal antibodies produced an additional decrease in cell viability of 7.4 units (95% CI: −5.7-20.5), this not being significantly different from the decrease observed with CD59 alone ($P = .269$). Finally, the cytotoxic effect produced when blocking with anti-CD59 directly correlated with the number of CD59 molecules per cell ($P < .001$).

Thus, in B-cell lymphoproliferative disorders, the cytotoxic effect of rituximab is mediated, at least in part, by the complement and is regulated by the number of CD20 and CD59 molecules per cell.

Induction of R-CDC in $CD20^{++}$ cells is not mediated by caspase activation and does not induce DNA cleavage

We investigated the implication of caspases in R-CDC in 4 $CD20^{++}$ cases (3 B-CLL and 1 MCL). Incubation of cells for 24 hours with rituximab+AB did not activate caspase-3, as determined by the absence of the active form of this protease by flow cytometry (Figure 4A). Furthermore, R-CDC was not associated with caspase-mediated nuclear features of apoptosis such as PARP proteolysis or DNA cleavage (appearance of the hypodiploid DNA peak) after 48 hours of incubation (Figure 4B,C). Finally, addition of 200 μM Z-VAD.fmk, a broad-spectrum caspase inhibitor, did not prevent phosphatydilserine exposure, cell shrinkage, and loss of $\Delta\Psi_m$ induced by rituximab+AB (Figure 4D). To discard the possibility that caspase activation occurred at earlier time points, we analyzed caspase-3 activation in 3 B-CLL sensitive cases following treatment with rituximab+AB for 1, 2, and 4 hours. No evidence of caspase activation was observed, whereas cells at these time points showed the typical features of cell death (data not shown). All these results indicate that the mechanism involved in R-CDC may occur in the absence of caspase activation.

R-CDC induces production of ROS

Since the cytotoxic effect of rituximab+AB was accompanied by a loss in $\Delta\Psi_m$, we tested whether this phenomenon was associated with the production of ROS. As seen in Figure 5A, incubation for 24 hours of $CD20^{++}$ cells from a representative MCL patient with rituximab+AB induced the production of ROS, as assessed by staining with DHE, a compound converted by O_2^- to highly fluorescent ethidium. Similar results were obtained in all the

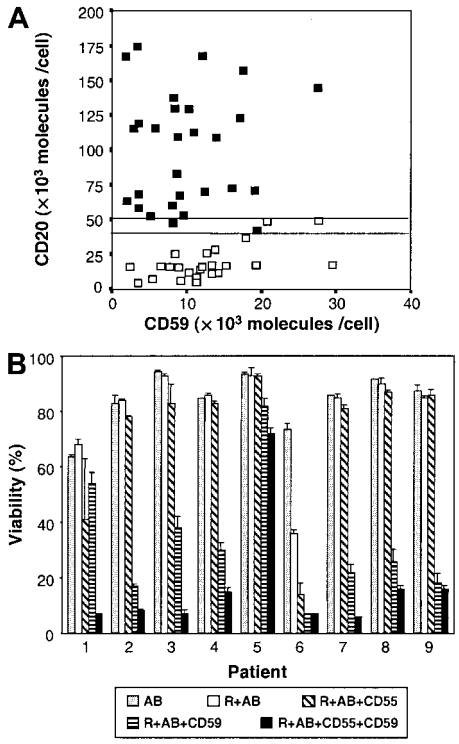

Figure 3. Role of CD59 expression in R-CDC. (A) Expression of CD20 and CD59 in cells from nonsensitive (□) and sensitive (■) patients. (B) Effect of CD55 and CD59 blockage on R-CDC. Cells from 9 B-CLL patients were incubated for 24 hours with 50 μg/mL rituximab and 10% AB (R+AB) alone or combined with anti-CD55 and/or anti-CD59. Cell viability was determined by annexin V binding as described in "Patients, materials, and methods."

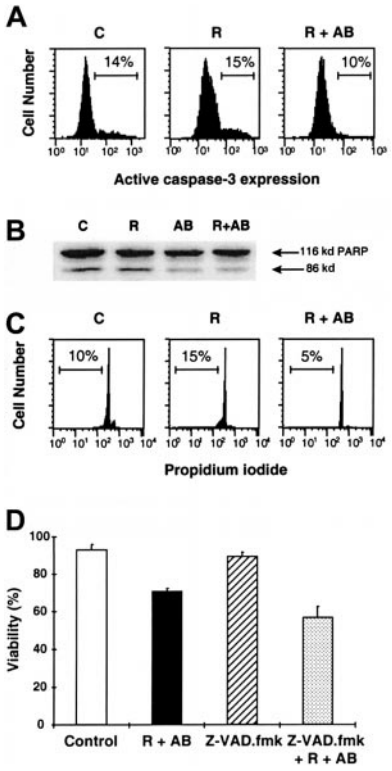

Figure 4. Complement-mediated R-CDC is not mediated by caspase activation. Cells of a representative CD20^{++} patient with B-CLL were incubated in medium alone (C), or with 50 μg/mL rituximab in the absence (R) or presence (R+AB) of 10% AB serum. (A) Analysis by flow cytometry of the active form of caspase-3 after 24 hours of incubation. (B) Analysis of PARP cleavage by Western blot after 48 hours of incubation. (C) Analysis of DNA content by staining with propidium iodide after 48 hours of incubation. (D) Effect of 200 μM Z-VAD.fmk on cell viability after 24 hours of incubation. Z-VAD.fmk was preincubated for 1 hour prior to the addition of the indicated factors. Cell viability was quantified by exposure of phosphatidylserine residues.

CD20^{++} cases sensitive to rituximab, with no differences according to the histology of the tumor.

To determine the implication of ROS in R-CDC, we incubated cells with rituximab+AB in the presence of 2 ROS scavengers. As shown in Figure 5B, incubation of cells from a representative CD20^{++} patient with Tiron, a pharmacologic cell-permeable scavenger of O_2^-, or the antioxidant NAC completely abolished the generation of ROS and reverted R-CDC, as analyzed by exposure of phosphatidylserine residues, changes in FSC/SSC pattern, and loss of $\Delta\Psi_m$. Similar results were obtained in cells from 5 additional patients. Moreover, we observed a dose-dependent inhibitory effect of Tiron (from 5 mM to 15 mM) and NAC (from 25 mM to 100 mM) that correlated with the number of CD20 molecules per cell (data not shown).

Finally, in order to establish the sequence of cellular changes induced by rituximab+AB, the kinetics of R-CDC were investigated in 4 CD20^{++} cases (1 B-CLL, 1 FL, 2 MCL). Addition of AB in cells preincubated with rituximab resulted in a rapid and intense detection of ROS, with maximal levels being achieved in less than 15 minutes (Figure 6A). As seen in Figure 6B, ROS production was accompanied by loss in $\Delta\psi_m$, which was detected as early as 2 minutes after the addition of AB. Exposure of phosphatidylserine residues was detected simultaneously to these changes in cells from CD20^{++} patients with high expression of CD20 molecules (Figure 6B, upper panel), but in cells from CD20^{++} patients with lower numbers of CD20 molecules (Figure 6B, lower panel), annexin V binding was observed later.

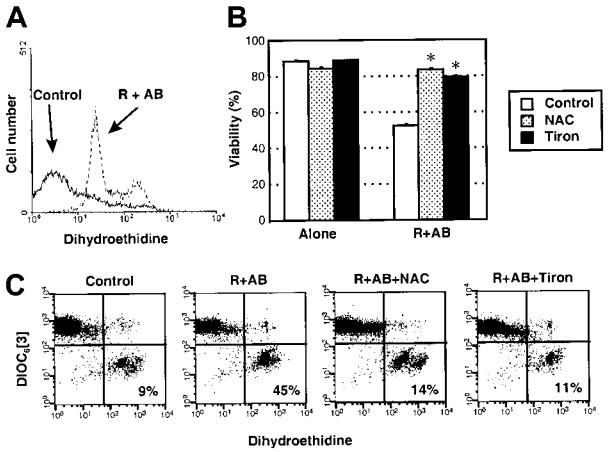

Figure 5. ROS production induced by rituximab+AB and effect of ROS scavengers. (A) Cells from a representative CD20^{++} patient with MCL were incubated for 24 hours in the presence (dashed line) or absence (solid line) of 50 μg/mL rituximab and 10% AB serum (R+AB) and stained with DHE. (B) Cells from a representative CD20^{++} patient with B-CLL were incubated for 20 hours with ROS scavengers (NAC, 25 mM; Tiron, 5 mM) in the absence or presence of rituximab and AB (R+AB). ROS scavengers were added one hour prior to the addition of rituximab and AB serum. Cell viability was determined by staining with annexin V binding. * Indicates $P < .05$. (C) The effect of ROS scavengers on $\Delta\Psi$m and ROS generation was quantified after 20 hours by dual staining with $DIOC_6$[3] and DHE.

Discussion

The results presented in this study show that the cytotoxic effect of rituximab on primary malignant B cells is, at least in part, complement mediated and that this process mainly occurs through the production of ROS. The generation of cytotoxic ROS in cells is due to the partial reduction of oxygen that leads to the generation of O_2^-. To avoid toxic cellular effects, this stable radical is enzymatically converted to other radicals such as hydroxyl (OH^-) and hydrogen peroxide (H_2O_2),[15] or rapidly reacts with nitric oxide (NO) yielding peroxynitrite ($ONOO^-$).[16] The production of ROS has a role in signal transduction and has been associated with many forms of apoptosis[17] as well as with the cell death that occurs in cerebrovascular accidents and neurodegenerative diseases.[18-22]

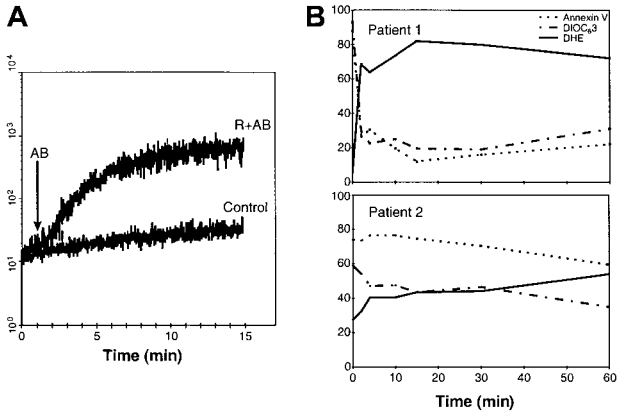

Figure 6. Kinetics of R-CDC–induced ROS production, loss of $\Delta\psi_m$, and phosphatidylserine exposure. (A) The kinetics of ROS generation were analyzed in cells from a patient with MCL with CD20^{++} expression (119×10^3 CD20 molecules/cell) as described in "Patients, materials, and methods." (B) Time-course of ROS production (solid line), loss of $\Delta\Psi_m$ (dashed line), and annexin V exposure (dotted line) in cells from a patient with MCL with very high levels of CD20 (137×10^3 molecules/cell) (top panel) and a CD20^{++} patient with B-CLL with high levels of CD20 (70×10^3 molecules/cell) (lower panel).

In the present study, we found a rapid and selective generation of ROS after the addition of rituximab and AB serum, since only specific scavengers of O_2^-, such as Tiron, and NAC completely reverted the production of ROS and all changes associated with cell death. Other ROS scavengers selective for H_2O_2 (glutathiome [GSH], catalase) and $ONOO^-$ (L-NAME, uric acid) produced a partial or no reversion on R-CDC (data not shown). Interestingly, the specific involvement of O_2^- has been recently described in the cytotoxic effect of estrogen derivates in B-CLL cells[23] and in the apoptosis of rat mesangial cells treated with tumor necrosis factor-α.[24]

Consistent with previous reports,[11] rituximab alone was unable to induce a cytotoxic effect on primary malignant B cells, the addition of a source of complement being necessary to obtain such an effect. Another mechanism that has been involved in the cytotoxic effect of rituximab is ADCC.[1,7] However, a previous report comparing specific rituximab-induced ADCC and CDC in several cell lines showed that CDC is more effective than ADCC.[7] Although CDC could be the major mechanism accounting for the elimination of circulating B lymphocytes following rituximab infusion, ADCC may contribute to the elimination of B cells in tissues where interaction between target and effector cells is higher.

Incubation of cells with rituximab and AB serum induced the typical cytoplasmic features of apoptosis: flow cytometric changes in FSC and SSC indicative of cell shrinkage, exposure of phosphatidylserine residues, and decrease in $\Delta\psi_m$. Neither caspase activation nor caspase-mediated nuclear features of apoptosis were observed and R-CDC was not blocked by the presence of the caspase inhibitor Z-VAD.fmk, indicating that R-CDC observed in primary malignant B cells occurred in the absence of caspase activation. A caspase-independent cell death has been described for treatment with several monoclonal antibodies,[25,26] and particularly, in B-CLL cells by CD47 ligation.[27] There are no extensive analyses of the pathways accounting for this sort of cell death but, interestingly, in some studies cell death was associated with ROS production and loss of $\Delta\Psi_m$,[25,28] as we have observed in R-CDC. In addition, it has been described that caspases are inhibited by oxidants[29,30] because, presumably, when the level of cytosolic ROS becomes too high, the essential cysteine in the active center of the caspases becomes oxidized or blocked.[31,32]

It has been described that rituximab induces a caspase-dependent apoptosis.[8,9,33] However, in all these studies in vitro crosslinking of rituximab with secondary antibodies was performed. The production of antibodies against rituximab has not been described in patients treated with rituximab; therefore, this mechanism is unlikely to occur in vivo.[2] Nevertheless, preliminary studies have suggested that caspases may be activated following in vivo infusion of rituximab,[34] therefore additional mechanisms could be involved in in vivo caspase activation. Although it has been described that some anti-CD20 antibodies can promote the activation of the Src-family kinases,[9] no implication of these kinases has been observed in our study. In fact, incubation with a selective inhibitor of this family of kinases (PP2) did not prevent R-CDC in cells from 4 of our cases (data not shown). Altogether, it is likely that many different pathways of cell death both dependent and independent of apoptosis could mediate the elimination of tumoral B cells in vivo.

We have observed that R-CDC directly correlates with the expression of the CD20 antigen in malignant B cells and a certain amount of antigen is required to trigger R-CDC. Therefore, the clinical differences in responses among patients with different types of B-lymphoproliferative disorders could be related, at least in part, to CD20 expression. Another factor influencing the response to rituximab is complement regulatory proteins. The blockage of CD59 with specific antibodies sensitized cells to rituximab, indicating that CD59, the protein controlling the membrane-attack complex, may have an important role in R-CDC. Similar results have been obtained in previous studies,[7] in contrast to others that proposed a major role for CD55.[11] These differences could be related to the different clones of monoclonal antibodies used to block cellular antigens.

The present results, obtained in primary malignant B cells, can serve as the basis for new therapeutic approaches that may improve the efficacy of rituximab in lymphoid malignancies. In this regard, it has been suggested that the up-regulation of CD20 on malignant B cells could enhance the effect of rituximab.[35-37] Additional strategies could involve the control of complement regulatory proteins on the surface of neoplastic B cells either by using bispecific monoclonal antibodies against both CD20 and CD59, to avoid side effects of a wide CD59 blockage, or by down-regulating the expression of CD59 with pharmacologic agents.[38,39]

In conclusion, this report provides evidence that CD20, CD59, and complement contribute to the in vitro cytotoxic effect of rituximab, with this being mediated by a caspase-independent process that involves ROS generation and loss of mitochondrial transmembrane potential. These results may be useful to establish a theoretical basis to improve the efficacy of therapy with rituximab.

Acknowledgment

We thank L. Quintó from the Unidad de Epidemiología y Bioestadística, Hospital Clínic, for his help in statistical analysis.

References

1. Reff ME, Carner K, Chambers KS, et al. Depletion of B cells in vivo by a chimeric mouse human monoclonal antibody to CD20. Blood. 1994;83: 435-445.
2. McLaughlin P, Grillo-Lopez AJ, Link BK, et al. Rituximab chimeric anti-CD20 monoclonal antibody therapy for relapsed indolent lymphoma: half of patients respond to a four-dose treatment program. J Clin Oncol. 1998;16:2825-2833.
3. Hainsworth JD, Burris HA III, Morrissey LH, et al. Rituximab monoclonal antibody as initial systemic therapy for patients with low-grade non-Hodgkin lymphoma. Blood. 2000;95:3052-3056.
4. Czuczman MS, Grillo-Lopez AJ, White CA, et al. Treatment of patients with low-grade B-cell lymphoma with the combination of chimeric anti-CD20 monoclonal antibody and CHOP chemotherapy. J Clin Oncol. 1999;17:268-276.
5. Foran JM, Rohatiner AZ, Cunningham D, et al. European phase II study of rituximab (chimeric anti-CD20 monoclonal antibody) for patients with newly diagnosed mantle-cell lymphoma and previously treated mantle-cell lymphoma, immunocytoma, and small B-cell lymphocytic lymphoma. J Clin Oncol. 2000;18:317-324.
6. Foran JM, Cunningham D, Coiffier B, et al. Treatment of mantle-cell lymphoma with rituximab (chimeric monoclonal anti-CD20 antibody): analysis of factors associated with response. Ann Oncol. 2000;11(suppl 1):117-121.
7. Harjunpaa A, Junnikkala S, Meri S. Rituximab (anti-CD20) therapy of B-cell lymphomas: direct complement killing is superior to cellular effector mechanisms. Scand J Immunol. 2000;51:634-641.
8. Shan D, Ledbetter JA, Press OW. Apoptosis of malignant human B cells by ligation of CD20 with monoclonal antibodies. Blood. 1998;91:1644-1652.
9. Hofmeister JK, Cooney D, Coggeshall KM. Clustered CD20 induced apoptosis: Src-family kinase, the proximal regulator of tyrosine phosphorylation, calcium influx, and caspase 3-dependent apoptosis. Blood Cells Mol Dis. 2000; 26:133-143.
10. Gorter A, Meri S. Immune evasion of tumor cells using membrane-bound complement regulatory proteins. Immunol Today. 1999;20:576-582.

11. Golay J, Zaffaroni L, Vaccari T, et al. Biologic response of B lymphoma cells to anti-CD20 monoclonal antibody rituximab in vitro: CD55 and CD59 regulate complement-mediated cell lysis. Blood. 2000;95:3900-3908.
12. Harris NL, Jaffe ES, Diebold J, et al. The World Health Organization classification of neoplastic diseases of the hematopoietic and lymphoid tissues: report of the Clinical Advisory Committee meeting, Airlie House, Virginia, November, 1997. Ann Oncol. 1999;10:1419-1432.
13. Bellosillo B, Villamor N, Colomer D, Pons G, Montserrat E, Gil J. In vitro evaluation of fludarabine in combination with cyclophosphamide and/or mitoxantrone in B-cell chronic lymphocytic leukemia. Blood. 1999;94:2836-2843.
14. Nicoletti I, Migliorati G, Pagliacci MC, Grignani F, Riccardi C. A rapid and simple method for measuring thymocyte apoptosis by propidium iodide staining and flow cytometry. J Immunol Methods. 1991;139:271-279.
15. Jacobson MD. Reactive oxygen species and programmed cell death. Trends Biochem Sci. 1996; 21:83-86.
16. Szabo C, Ohshima H. DNA damage induced by peroxynitrite: subsequent biological effects. Nitric Oxide. 1997;1:373-385.
17. Suzuki YJ, Forman HJ, Sevanian A. Oxidants as stimulators of signal transduction. Free Radic Biol Med. 1997;22:269-285.
18. Tan S, Sagara Y, Liu Y, Maher P, Schubert D. The regulation of reactive oxygen species production during programmed cell death. J Cell Biol. 1998; 141:1423-1432.
19. Shigenaga MK, Hagen TM, Ames BN. Oxidative damage and mitochondrial decay in aging. Proc Natl Acad Sci U S A. 1994;91:10771-10778.
20. Knight JA. Reactive oxygen species and the neurodegenerative disorders. Ann Clin Lab Sci. 1997; 27:11-25.
21. Halliwell B. Reactive oxygen species and the central nervous system. J Neurochem. 1992;59: 1609-1623.
22. Ames BN, Shigenaga MK, Hagen TM. Oxidants, antioxidants, and the degenerative diseases of aging. Proc Natl Acad Sci U S A. 1993;90:7915-7922.
23. Huang P, Feng L, Oldham EA, Keating MJ, Plunkett W. Superoxide dismutase as a target for the selective killing of cancer cells. Nature. 2000;407: 390-395.
24. Moreno-Manzano V, Ishikawa Y, Lucio-Cazana J, Kitamura M. Selective involvement of superoxide anion, but not downstream compounds hydrogen peroxide and peroxynitrite, in tumor necrosis factor-alpha-induced apoptosis of rat mesangial cells. J Biol Chem. 2000;275:12684-12691.
25. Lesage S, Steff AM, Philippoussis F, et al. CD4+CD8+ thymocytes are preferentially induced to die following CD45 cross-linking, through a novel apoptotic pathway. J Immunol. 1997;159:4762-4771.
26. Deas O, Dumont C, MacFarlane M, et al. Caspase-independent cell death induced by anti-CD2 or staurosporine in activated human peripheral T lymphocytes. J Immunol. 1998;161:3375-3383.
27. Mateo V, Lagneaux L, Bron D, et al. CD47 ligation induces caspase-independent cell death in chronic lymphocytic leukemia. Nat Med. 1999;5: 1277-1284.
28. Xiang J, Chao DT, Korsmeyer SJ. BAX-induced cell death may not require interleukin 1 beta-converting enzyme-like proteases. Proc Natl Acad Sci U S A. 1996;93:14559-14563.
29. Cai J, Jones DP. Superoxide in apoptosis: mitochondrial generation triggered by cytochrome c loss. J Biol Chem. 1998;273:11401-11404.
30. Fiers W, Beyaert R, Declercq W, Vandenabeele P. More than one way to die: apoptosis, necrosis and reactive oxygen damage. Oncogene. 1999; 18:7719-7730.
31. Ueda S, Nakamura H, Masutani H, et al. Redox regulation of caspase-3(-like) protease activity: regulatory roles of thioredoxin and cytochrome c. J Immunol. 1998;161:6689-6695.
32. Hampton MB, Orrenius S. Redox regulation of apoptotic cell death in the immune system. Toxicol Lett. 1998;102-103:355-358.
33. Shan D, Ledbetter JA, Press OW. Signaling events involved in anti-CD20-induced apoptosis of malignant human B cells. Cancer Immunol Immunother. 2000;48:673-683.
34. Reed JC. Apoptosis and cancer: strategies for integrating programmed cell death. Semin Hematol. 2000;37(suppl 7):9-16.
35. Sivaraman S, Venugopal P, Ranganathan R, et al. Effect of interferon-alpha on CD20 antigen expression of B-cell chronic lymphocytic leukemia. Cytokines Cell Mol Ther. 2000;6:81-87.
36. Venugopal P, Sivaraman S, Huang XK, Nayini J, Gregory SA, Preisler HD. Effects of cytokines on CD20 antigen expression on tumor cells from patients with chronic lymphocytic leukemia. Leuk Res. 2000;24:411-415.
37. Treon SP, Shima Y, Grossbard ML, et al. Treatment of multiple myeloma by antibody mediated immunotherapy and induction of myeloma selective antigens. Ann Oncol. 2000;11(suppl 1):107-111.
38. Bjorge L, Matre R. Down-regulation of CD59 (protectin) expression on human colorectal adenocarcinoma cell lines by levamisole. Scand J Immunol. 1995;42:512-516.
39. Honeychurch J, Tutt AL, Valerius T, Heijnen IA, Van De Winkel JG, Glennie MJ. Therapeutic efficacy of FcγRI/CD64-directed bispecific antibodies in B-cell lymphoma. Blood. 2000;96:3544-3552.